Stockholms universitet

Oskar Klein centre

Knut and Alice Wallenberg Foundation

Lyman-alpha profiles from z=0 to 11

Exploring the inside of ionized bubbles, the evolution of the IGM, and the buildup of galaxy winds

Matthew Hα-YES
Stockholm University, Dept of Astronomy
Oskar Klein Centre for Cosmoparticle Physics

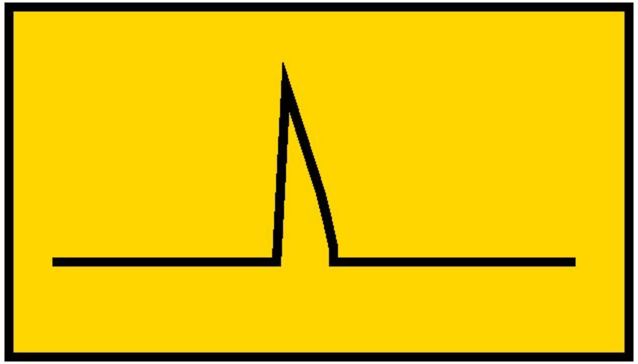

With: Claudia Scarlata (UMN), Axel Runnholm (SU),
Max Gronke (MPE), T. Emil Rivera-Thorsen (SU)

Lyman-* CreteMeet 2023, Κολυμβαρι (LGP!)

Objectives and contents

- **Study of low-redshift Lya emitters**
  - Sample overview
  - Lya output with properties of stars & gas
  - Evolution & acceleration of galaxy winds

- **Evolution of profiles with redshift**
  - Intrinsic LAE profiles do not evolve significantly
  - IGM is responsible for reshaping Lya

- **Lya profiles to infer IGM properties during the EoR**
  - Derive sizes of ionized regions
  - Estimate the LyC escape fraction

Objectives and contents

- **Study of low-redshift Lya emitters**
    - Sample overview
    - Lya output with properties of stars & gas
    - Evolution & acceleration of galaxy winds

Hayes et al 2023
MNRAS, 520, 5903

Hayes 2023
MNRAS, 519, 26

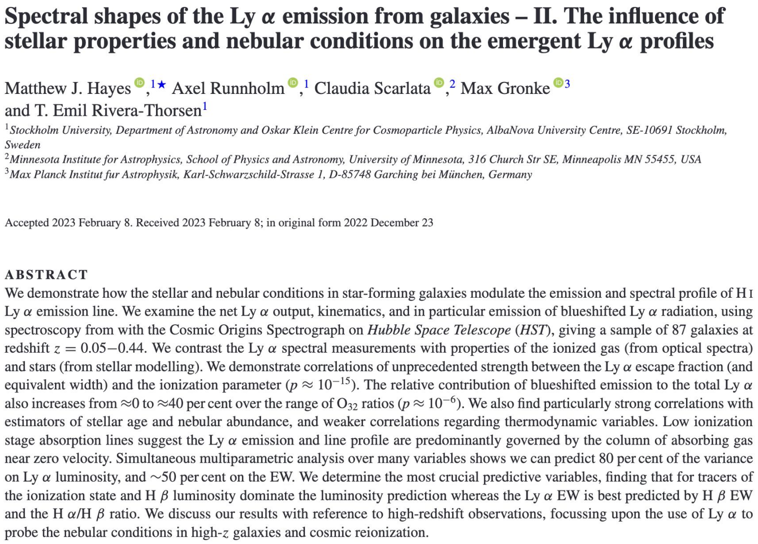

Spectral shapes of the Ly α emission from galaxies – II. The influence of stellar properties and nebular conditions on the emergent Ly α profiles

Matthew J. Hayes[1]★ Axel Runnholm[1] Claudia Scarlata[2] Max Gronke[3]
and T. Emil Rivera-Thorsen[1]
[1] *Stockholm University, Department of Astronomy and Oskar Klein Centre for Cosmoparticle Physics, AlbaNova University Centre, SE-10691 Stockholm, Sweden*
[2] *Minnesota Institute for Astrophysics, School of Physics and Astronomy, University of Minnesota, 316 Church Str SE, Minneapolis MN 55455, USA*
[3] *Max Planck Institut fur Astrophysik, Karl-Schwarzschild-Strasse 1, D-85748 Garching bei München, Germany*

Accepted 2023 February 8. Received 2023 February 8; in original form 2022 December 23

ABSTRACT

We demonstrate how the stellar and nebular conditions in star-forming galaxies modulate the emission and spectral profile of H I Ly α emission line. We examine the net Ly α output, kinematics, and in particular emission of blueshifted Ly α radiation, using spectroscopy from with the Cosmic Origins Spectrograph on *Hubble Space Telescope* (*HST*), giving a sample of 87 galaxies at redshift $z = 0.05-0.44$. We contrast the Ly α spectral measurements with properties of the ionized gas (from optical spectra) and stars (from stellar modelling). We demonstrate correlations of unprecedented strength between the Ly α escape fraction (and equivalent width) and the ionization parameter ($p \approx 10^{-15}$). The relative contribution of blueshifted emission to the total Ly α also increases from $\approx$0 to $\approx$40 per cent over the range of O_{32} ratios ($p \approx 10^{-6}$). We also find particularly strong correlations with estimators of stellar age and nebular abundance, and weaker correlations regarding thermodynamic variables. Low ionization stage absorption lines suggest the Ly α emission and line profile are predominantly governed by the column of absorbing gas near zero velocity. Simultaneous multiparametric analysis over many variables shows we can predict 80 per cent of the variance on Ly α luminosity, and $\sim$50 per cent on the EW. We determine the most crucial predictive variables, finding that for tracers of the ionization state and H β luminosity dominate the luminosity prediction whereas the Ly α EW is best predicted by H β EW and the H α/H β ratio. We discuss our results with reference to high-redshift observations, focussing upon the use of Ly α to probe the nebular conditions in high-z galaxies and cosmic reionization.

Accelerating galaxy winds during the big bang of starbursts

Matthew. J. Hayes★
Stockholm University, Department of Astronomy and Oskar Klein Centre for Cosmoparticle Physics, AlbaNova University Centre, SE-10691, Stockholm, Sweden

Accepted 2022 October 20. Received 2022 October 19; in original form 2022 July 8

ABSTRACT

We develop a new method to infer the temporal, geometric, and energetic properties of galaxy outflows, by combining stellar spectral modelling to infer starburst ages, and absorption lines to measure velocities. If winds are accelerated with time during a starburst event, then these two measurements enable us to solve for the wind radius, similarly to length-scales and the Hubble parameter in big bang cosmology. This wind radius is the vital, but hard-to-constrain parameter in wind physics. We demonstrate the method using spectra of 87 starburst galaxies at $z = 0.05 - 0.44$, finding that winds accelerate throughout the starburst phase and grow to typical radii of $\approx$1 kpc in $\approx$10 Myr. Mass flow rates increase rapidly with time, and the mass-loading factor exceeds unity at about 10 Myr – while still being accelerated, the gas will likely unbind from the local potential and enrich the circumgalactic medium. We model the mechanical energy available from stellar winds and supernovae, and estimate that a negligible amount is accounted for in the cool outflow at early times. However, the energy deposition increases rapidly and $\sim$10 per cent of the budget is accounted for in the cool flow at 10 Myr, similar to some recent hydrodynamical simulations. We discuss how this model can be developed, especially for high-redshift galaxies.

Key words: ultraviolet: galaxies – galaxies: starburst – galaxies: kinematics and dynamics.

Sample: the entire COS archive of galaxies, minus a few…

Library of mid-resolution spectra at z > ~0.02

- LARS/eLARS/Lya Halos: x3 programs
- Henry: Green Peas + MgII emitters
- Wofford: x2 HII galaxies
- Scarlata: GALEX LAEs
- Heckman: Lyman break analogs. x3 progs.
- Thuan/Izotov: GP-like, LyC cand. x4 progs.
- Malhotra: blueberries
- Jaskot: GPs

~150 galaxies with **Lyα** and **some UV**
Cut at z>0.05 for ‘global’ Lyα ⇒ 87 galaxies

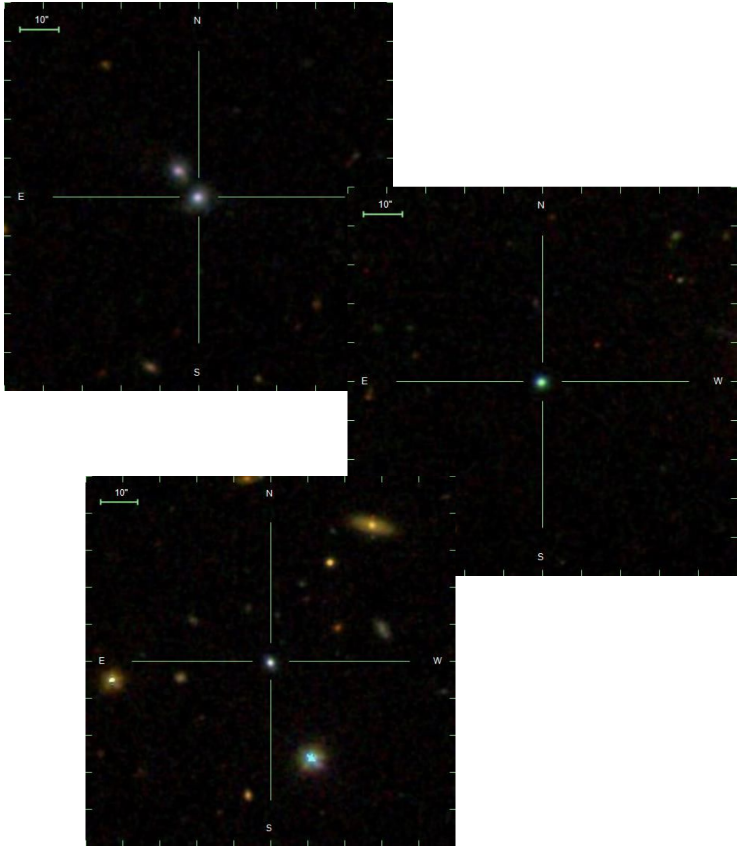

Stage I: Model the UV spectrum

Model with population synthesis
Multiple instantaneous bursts

Derive age, Z, SFH, SN rate, …

Subtract continuum: measure 42 optical emission lines

Derive: A_V, ionization param, …

Normalize continuum: measure ISM absorption lines: 11 lines of 7 ions

Derive: column density, velocities

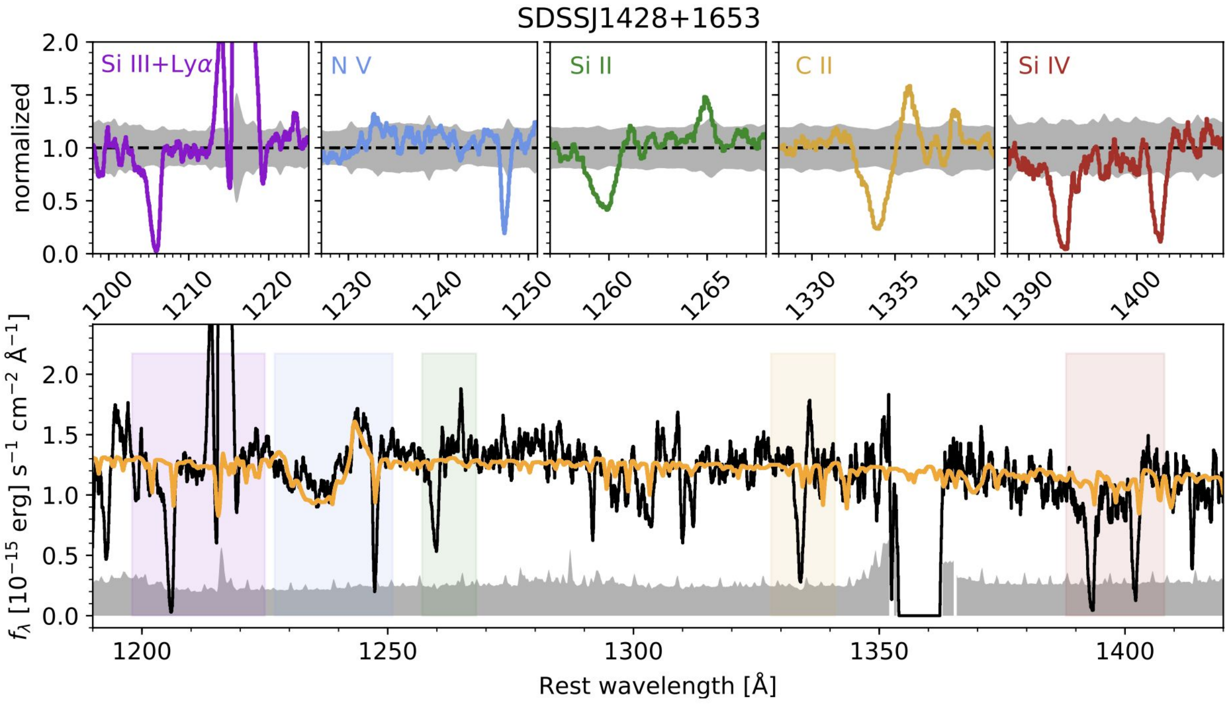

Measure the Lyα profiles

LYMAN ALPHA
SPECTRAL DATABASE

Measures 39 properties of the Lyα

- Fluxes, flux densities, peaks
- Troughs
- Velocities of peaks
- Skewness
- Blue and red sides
- z_{sys} given AND estimated from Lyα

Runnholm, Gronke & MH 2021

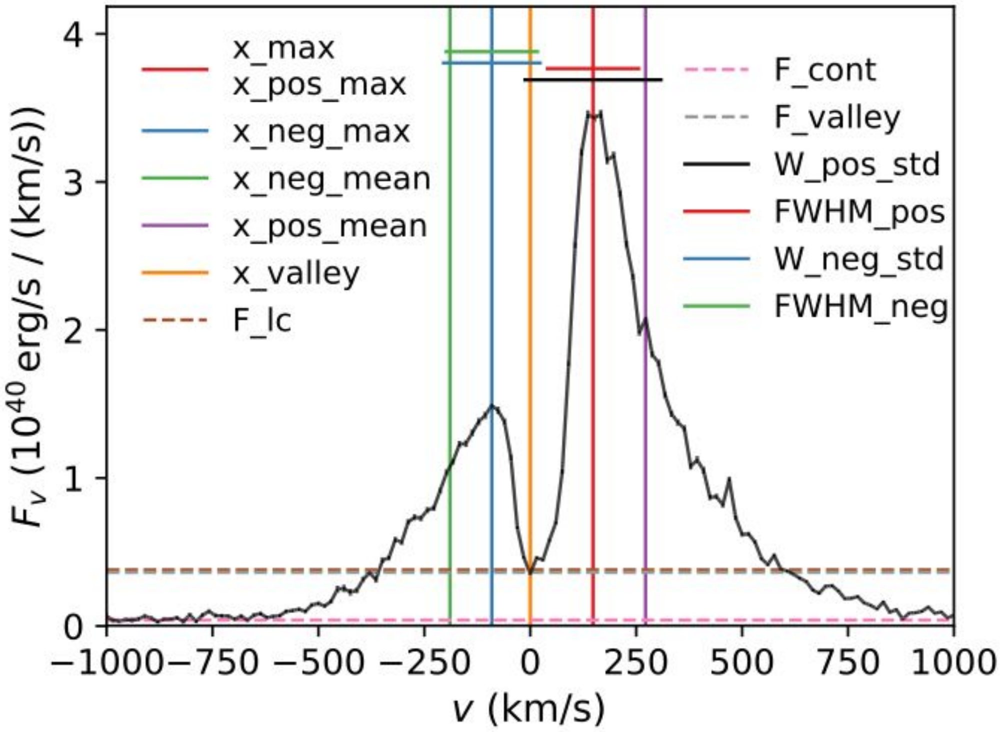

Characteristics

Ionizing properties
with stellar age

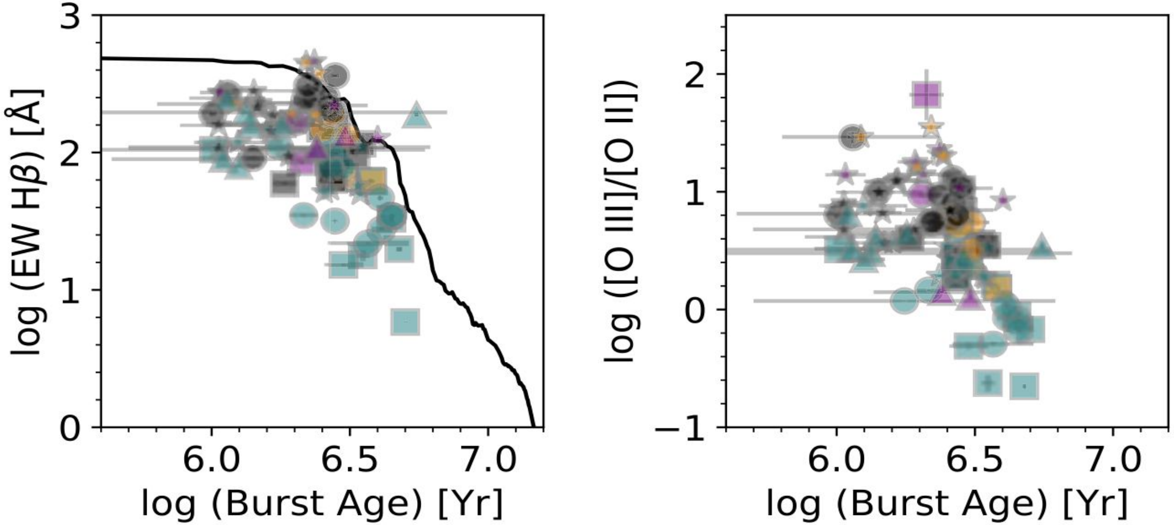

BPT and excitation
diagnostic diagrams

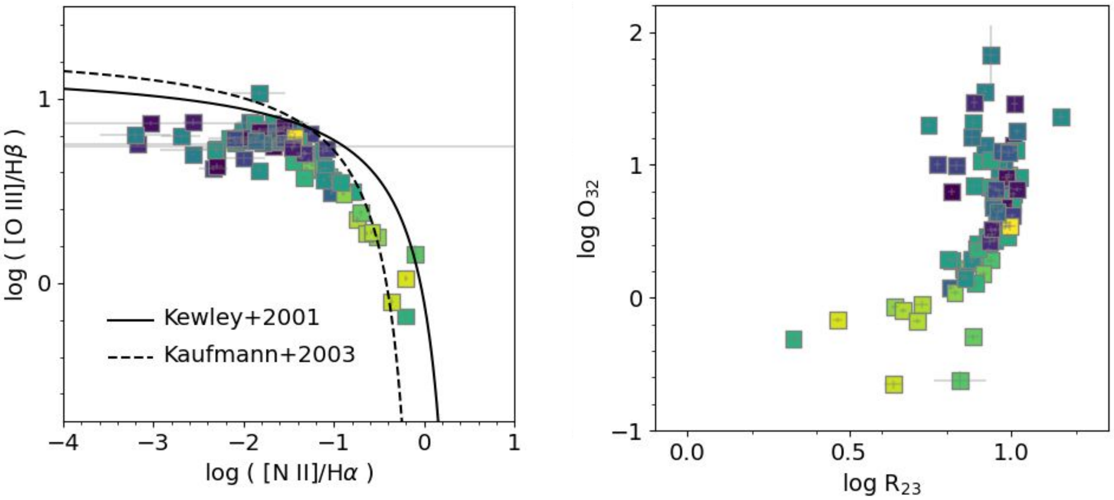

Global Lya output

Strong Lya variation at high mass & SFR

Upper envelope set by expectations

Anticorrelations with the usual scatter

Interesting, but already known…

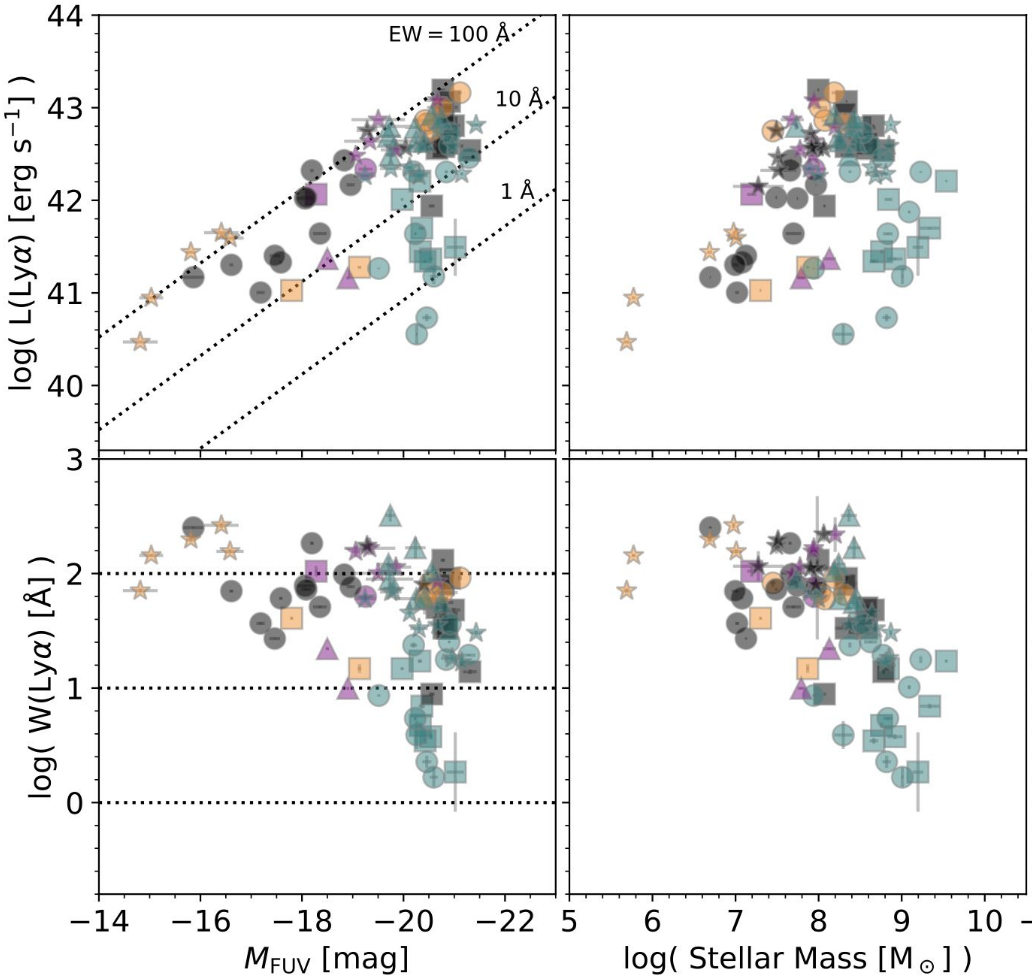

Bin by age, and stack…

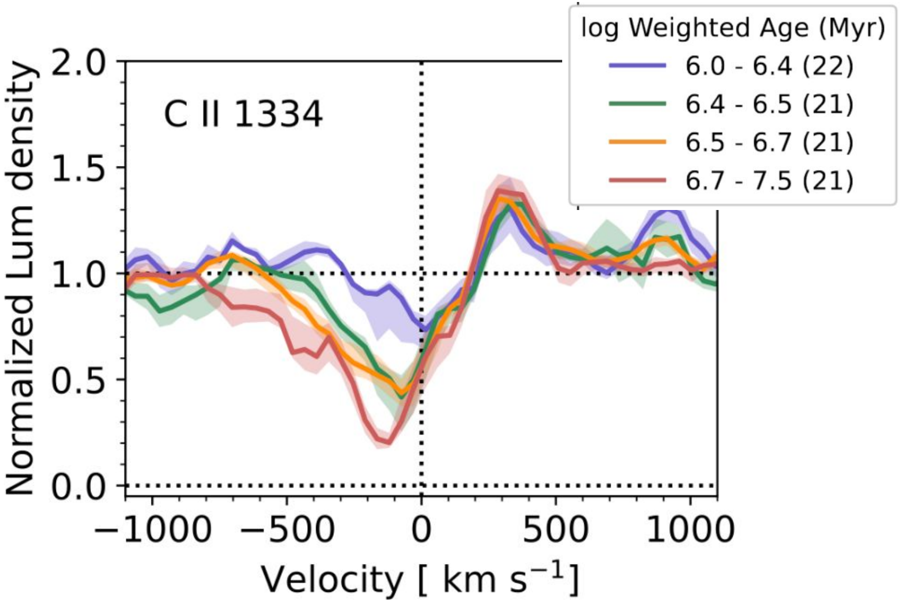

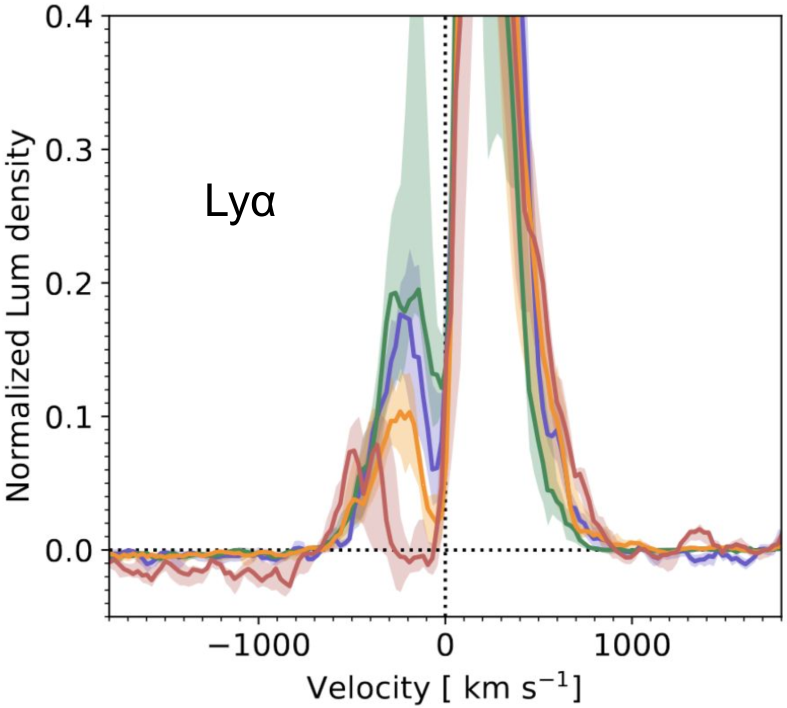

CII: cool gas in expanding envelope. Absorption gets stronger & faster with time

Lya: transfers through this expanding medium. Blue peak gets weaker and bluer

Envelope expands and accelerates with time

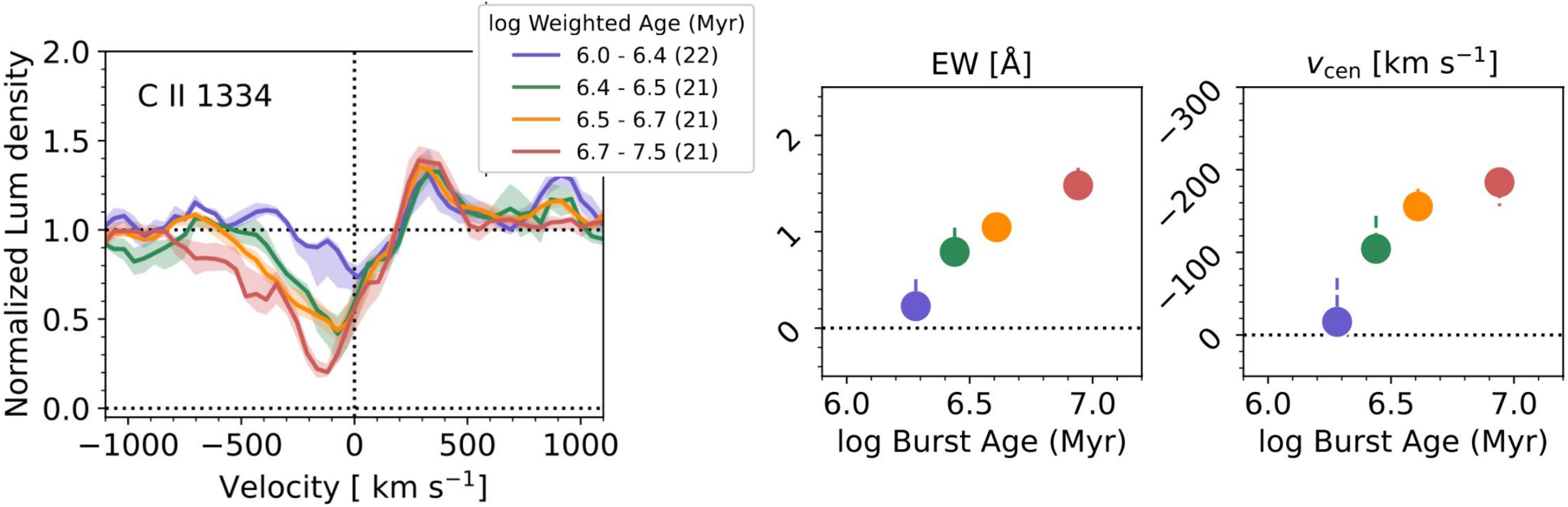

CII: cool gas in expanding envelope.   Absorption gets stronger & faster with time

Lya: transfers through this expanding medium. Blue peak gets weaker and bluer

More gas condenses or is advected into wind

Wind Flow and Structure

Wind structure

- Observed to get faster with time

  Looks like wind is accelerated

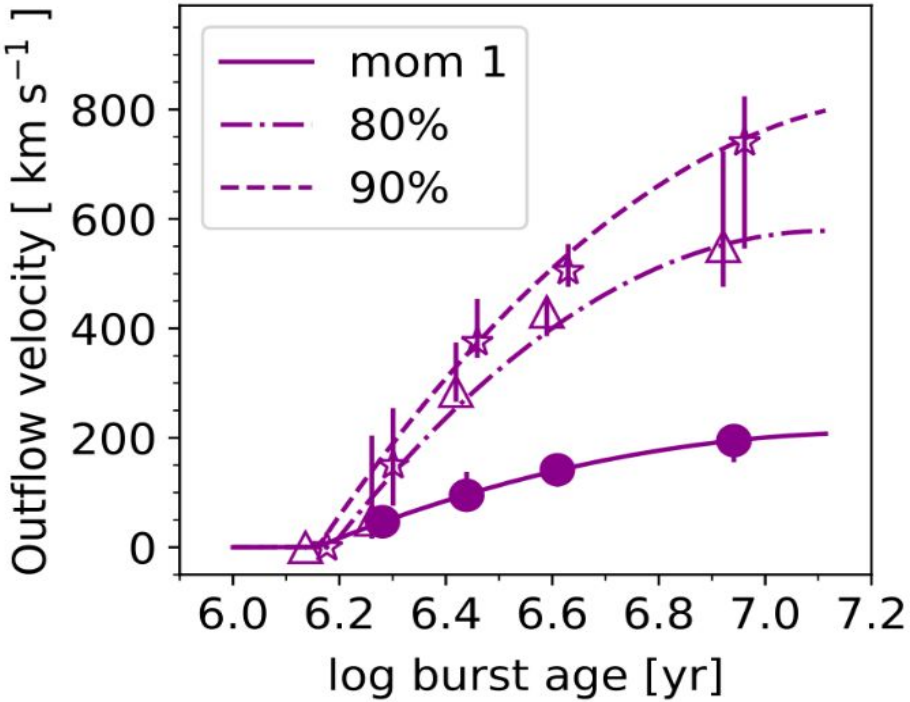

Wind Flow and Structure

Wind structure

- Observed to get faster with time

  Looks like wind is accelerated

- More cool gas found in wind

  Alternatively: gas condensed out

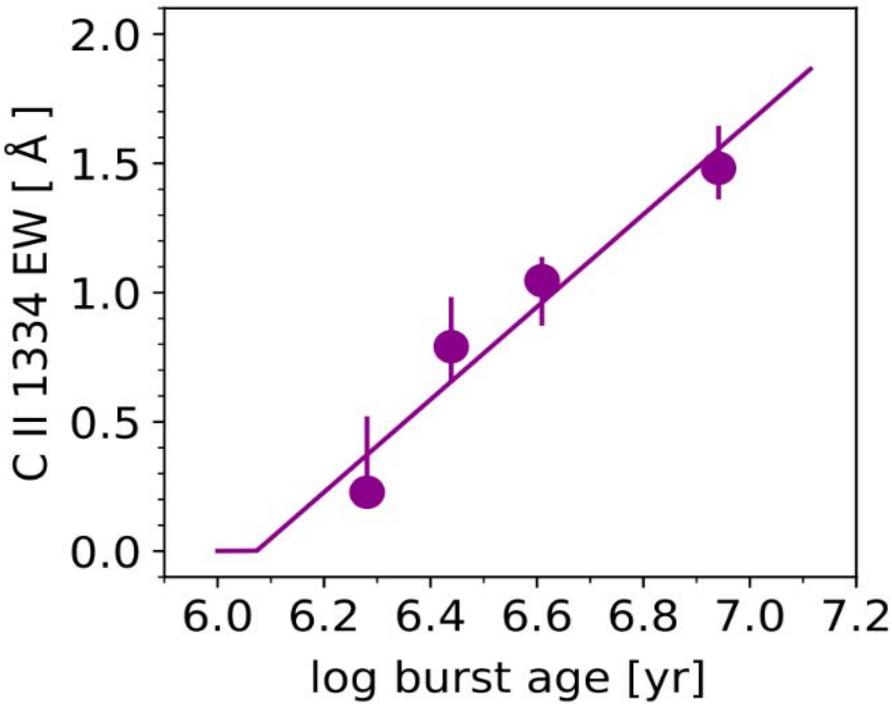

Wind Flow and Structure

Wind structure

- Observed to get faster with time

  Looks like wind is accelerated

- More cool gas found in wind

  Alternatively: gas condensed out

$$\boxed{r_{\text{wind}}(t) = \int_0^{t_{\text{obs}}} v_{\text{wind}}(t)\,dt}$$

- Bulk reaches ~1 kpc in ~10 Myr

  Wind is ‘stretched’ with time.

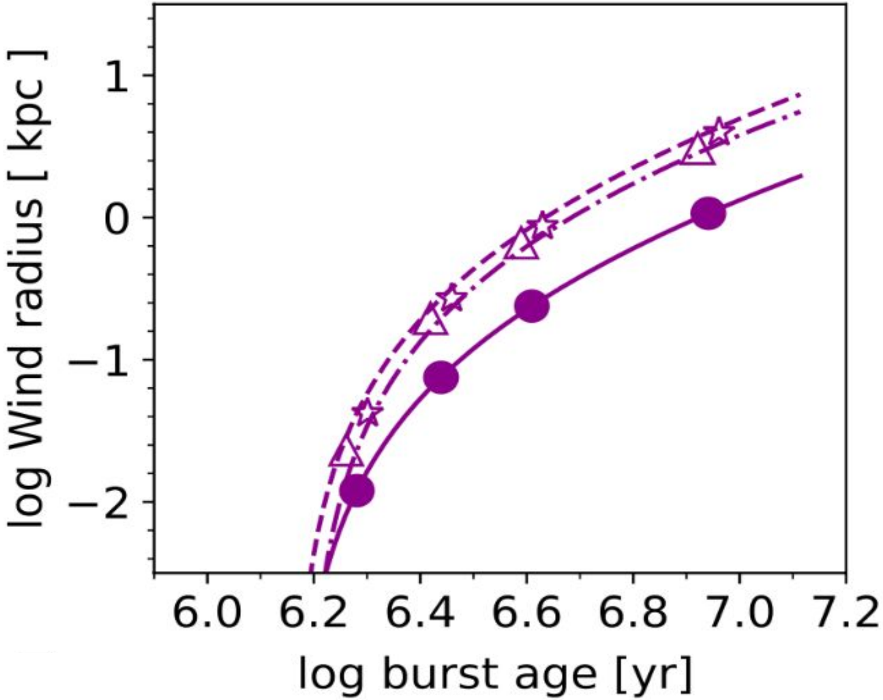

Wind mass & Outflow Energetics

$$M_{\rm wind} = 4\pi r^2_{\rm wind} f_{\rm cov} N_{\rm H} m_{\rm H} \mu$$

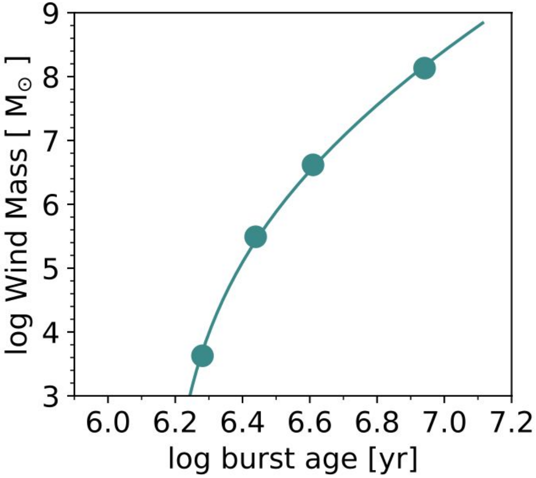

Wind mass

Starts at nothing

Reach 10^8 Msun @ 10Myr

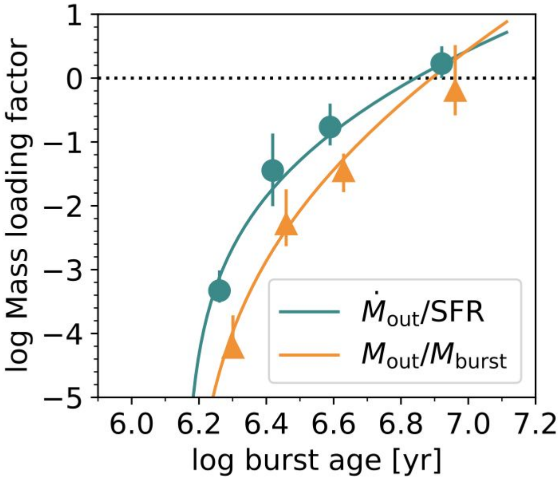

Mass loading factor

$$\eta \equiv \dot{M}_{\rm out}/{\rm SFR}$$

Exceeds 1 after 10 Myr

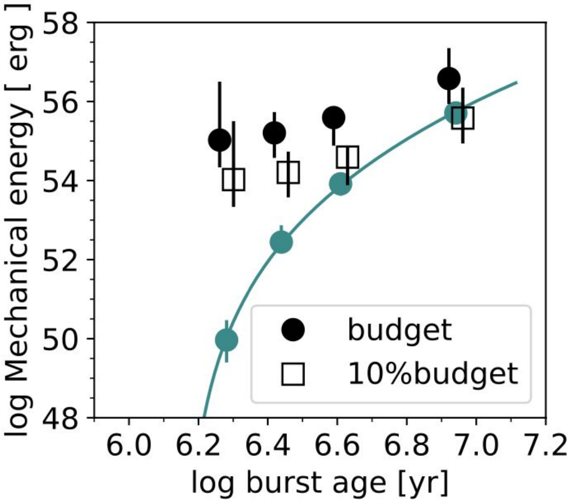

Mechanical energy

Reaches 10^{56} erg in 10 Myr

~10^5 SNe

Stellar feedback: ~10x more

All increase with time

Lya vs [O III] / [O II]

At higher O_{32} you get:

1. More blueshifted emission
   ~0 at O_{32} ~ 1
   ~30% at O_{32} ~ 10

2. Narrower peaks
   More emission near v = 0

3. More Lya: EW and fesc

Higher ionization conditions in young bursts allows the Lya to escape

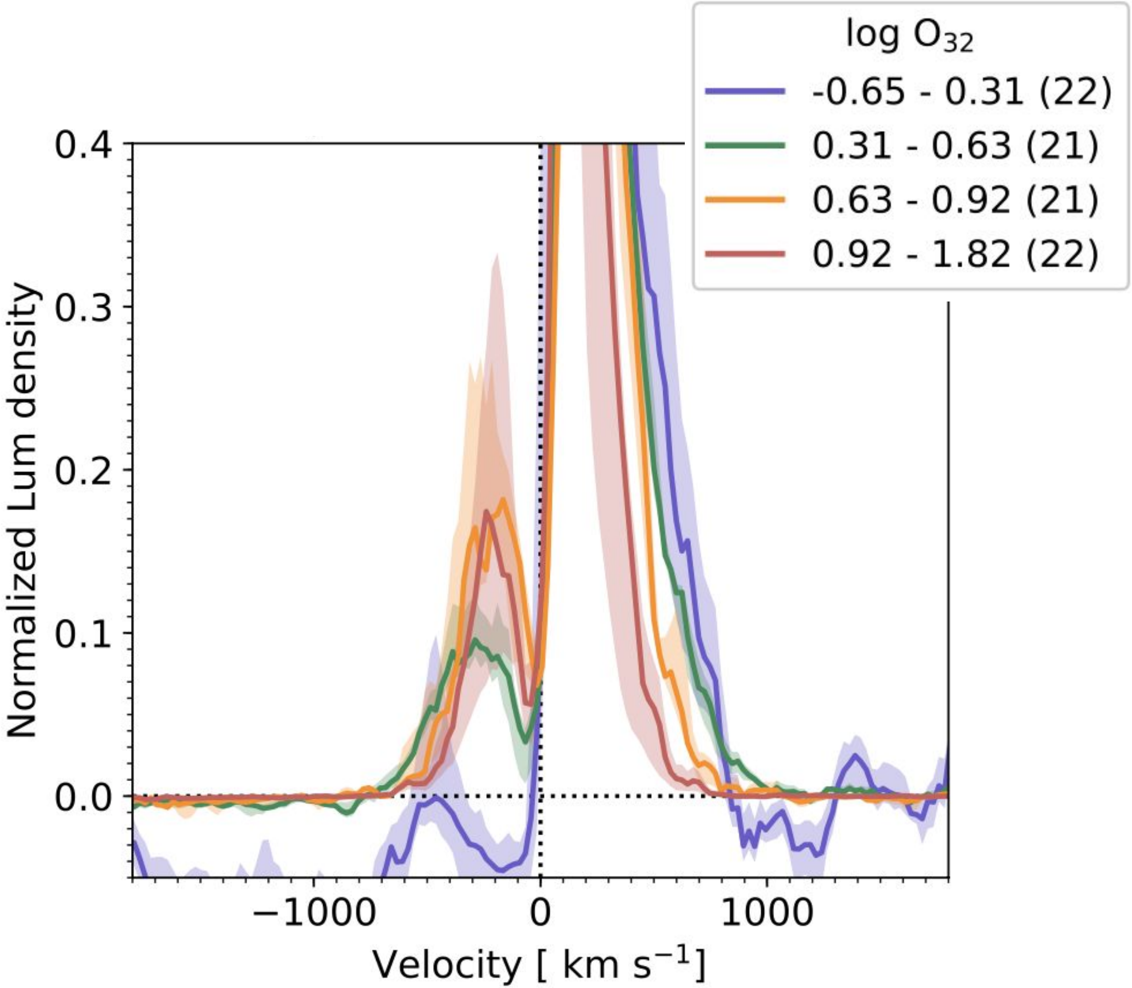

Lya vs [O III] / [O II]

At higher O_{32} you get:

1. More blueshifted emission
   ~0 at O_{32} ~ 1
   ~30% at O_{32} ~ 10

2. Narrower peaks
   More emission near v = 0

3. More Lya: EW and fesc

Higher ionization conditions in young bursts allows the Lya to escape

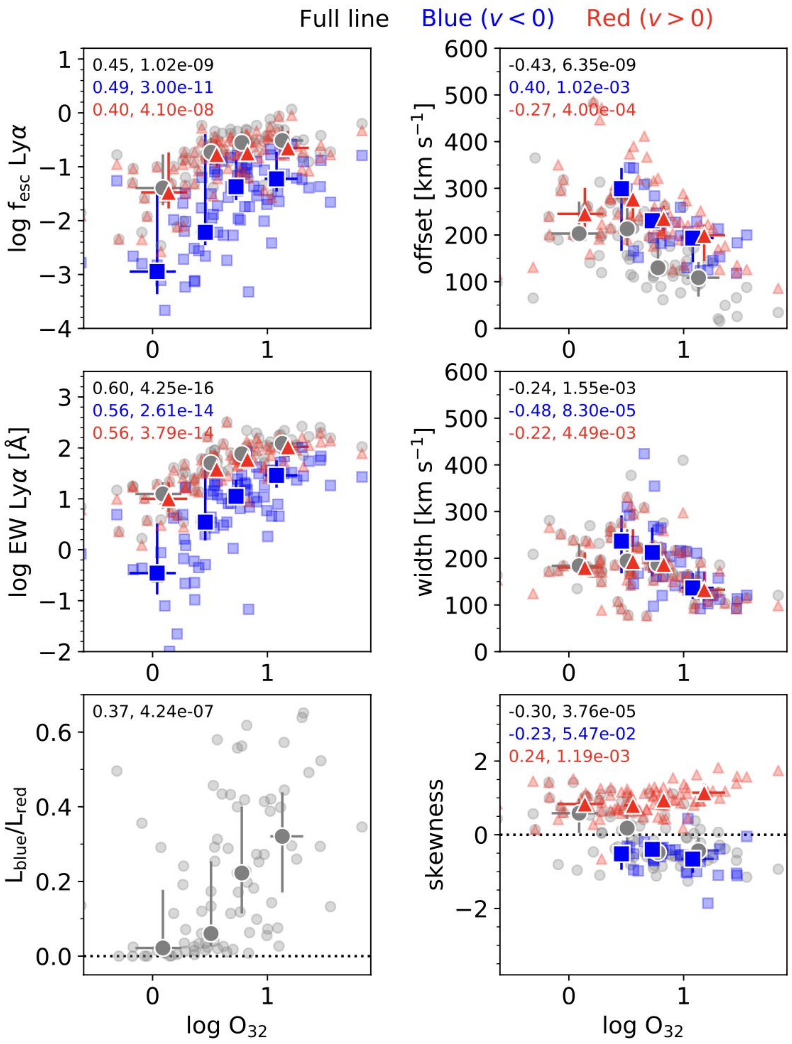

Lya with nebular properties

Kendall's τ and associated *p*-value

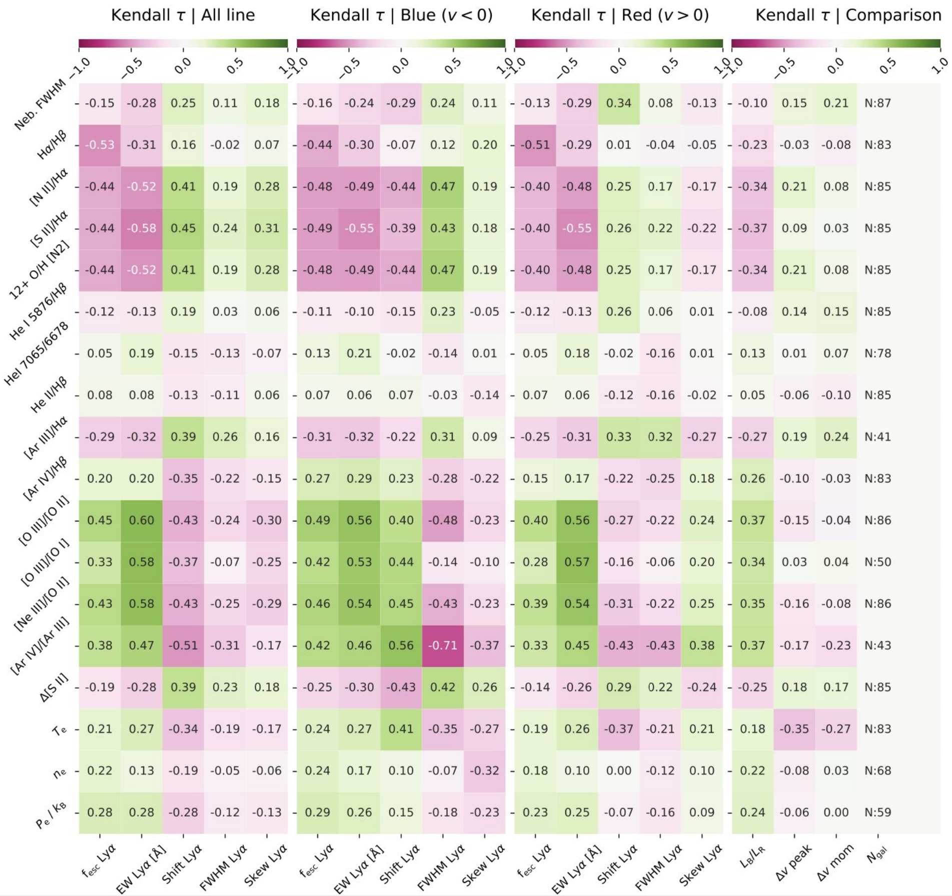

	Kendall τ | All line					Kendall τ | Blue ($v<0$)					Kendall τ | Red ($v>0$)					Kendall τ | Comparison			
	f_{esc} Lyα	EW Lyα [Å]	Shift Lyα	FWHM Lyα	Skew Lyα	f_{esc} Lyα	EW Lyα [Å]	Shift Lyα	FWHM Lyα	Skew Lyα	f_{esc} Lyα	EW Lyα [Å]	Shift Lyα	FWHM Lyα	Skew Lyα	L_B/L_R	Δv peak	Δv mom	N_{gal}
Neb. FWHM	-0.15	-0.28	0.25	0.11	0.18	-0.16	-0.24	-0.29	0.24	0.11	-0.13	-0.29	0.34	0.08	-0.13	-0.10	0.15	0.21	N:87
Hα/Hβ	-0.53	-0.31	0.16	-0.02	0.07	-0.44	-0.30	-0.07	0.12	0.20	-0.51	-0.29	0.01	-0.04	-0.05	-0.23	-0.03	-0.08	N:83
[N II]/Hα	-0.44	-0.52	0.41	0.19	0.28	-0.48	-0.49	-0.44	0.47	0.19	-0.40	-0.48	0.25	0.17	-0.17	-0.34	0.21	0.08	N:85
[S II]/Hα	-0.44	-0.58	0.45	0.24	0.31	-0.49	-0.55	-0.39	0.43	0.18	-0.40	-0.55	0.26	0.22	-0.22	-0.37	0.09	0.03	N:85
12+ O/H [N2]	-0.44	-0.52	0.41	0.19	0.28	-0.48	-0.49	-0.44	0.47	0.19	-0.40	-0.48	0.25	0.17	-0.17	-0.34	0.21	0.08	N:85
He I 5876/Hβ	-0.12	-0.13	0.19	0.03	0.06	-0.11	-0.10	-0.15	0.23	-0.05	-0.12	-0.13	0.26	0.06	0.01	-0.08	0.14	0.15	N:85
HeI 7065/6678	0.05	0.19	-0.15	-0.13	-0.07	0.13	0.21	-0.02	-0.14	0.01	0.05	0.18	-0.02	-0.16	0.01	0.13	0.01	0.07	N:78
He II/Hβ	0.08	0.08	-0.13	-0.11	0.06	0.07	0.06	0.07	-0.03	-0.14	0.07	0.06	-0.12	-0.16	-0.02	0.05	-0.06	-0.10	N:85
[Ar III]/Hα	-0.29	-0.32	0.39	0.26	0.16	-0.31	-0.32	-0.22	0.31	0.09	-0.25	-0.31	0.33	0.32	-0.27	-0.27	0.19	0.24	N:41
[Ar IV]/Hβ	0.20	0.20	-0.35	-0.22	-0.15	0.27	0.29	0.23	-0.28	-0.22	0.15	0.17	-0.22	-0.25	0.18	0.26	-0.10	-0.03	N:83
[O III]/[O II]	0.45	0.60	-0.43	-0.24	-0.30	0.49	0.56	0.40	-0.48	-0.23	0.40	0.56	-0.27	-0.22	0.24	0.37	-0.15	-0.04	N:86
[O III]/[O I]	0.33	0.58	-0.37	-0.07	-0.25	0.42	0.53	0.44	-0.14	-0.10	0.28	0.57	-0.16	-0.06	0.20	0.34	0.03	0.04	N:50
[Ne III]/[O II]	0.43	0.58	-0.43	-0.25	-0.29	0.46	0.54	0.45	-0.43	-0.23	0.39	0.54	-0.31	-0.22	0.25	0.35	-0.16	-0.08	N:86
[Ar IV]/[Ar III]	0.38	0.47	-0.51	-0.31	-0.17	0.42	0.46	0.56	-0.71	-0.37	0.33	0.45	-0.43	-0.43	0.38	0.37	-0.17	-0.23	N:43
Δ[S II]	-0.19	-0.28	0.39	0.23	0.18	-0.25	-0.30	-0.43	0.42	0.26	-0.14	-0.26	0.29	0.22	-0.24	-0.25	0.18	0.17	N:85
T_e	0.21	0.27	-0.34	-0.19	-0.17	0.24	0.27	0.41	-0.35	-0.27	0.19	0.26	-0.37	-0.21	0.21	0.18	-0.35	-0.27	N:83
n_e	0.22	0.13	-0.19	-0.05	-0.06	0.24	0.17	0.10	-0.07	-0.32	0.18	0.10	0.00	-0.12	0.10	0.22	-0.08	0.03	N:68
P_e / k_B	0.28	0.28	-0.28	-0.12	-0.13	0.29	0.26	0.15	-0.18	-0.23	0.23	0.25	-0.07	-0.16	0.09	0.24	-0.06	0.00	N:59

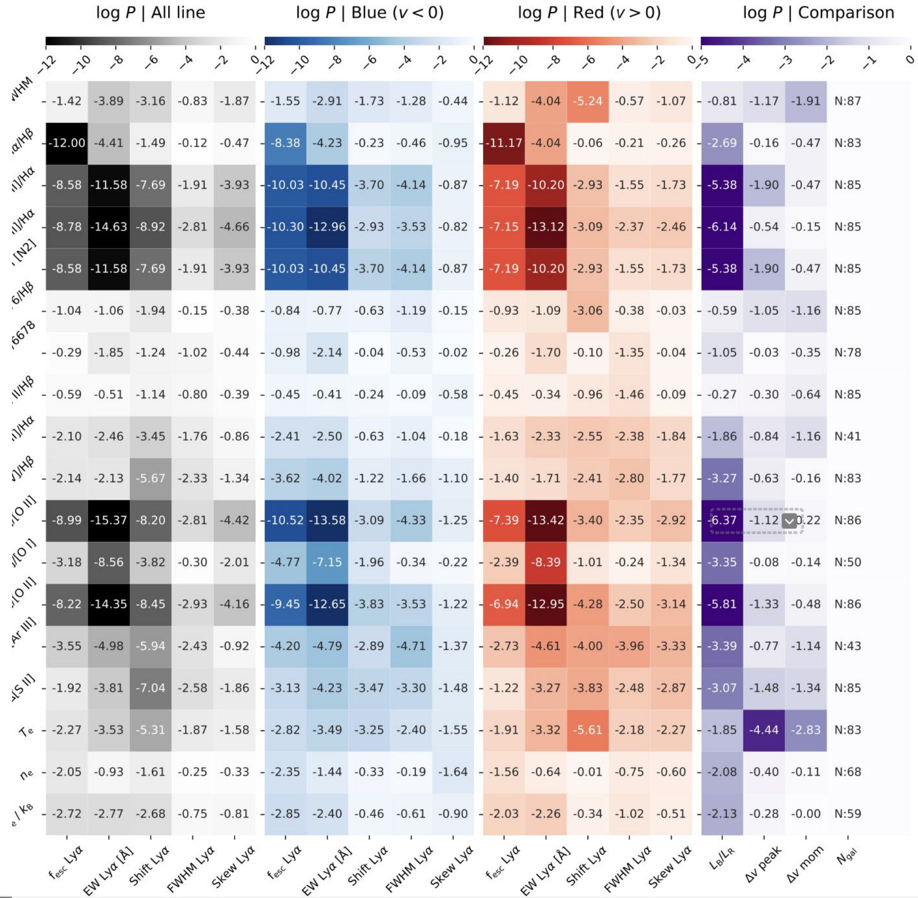

	log P | All line					log P | Blue ($v<0$)					log P | Red ($v>0$)					log P | Comparison			
	f_{esc} Lyα	EW Lyα [Å]	Shift Lyα	FWHM Lyα	Skew Lyα	f_{esc} Lyα	EW Lyα [Å]	Shift Lyα	FWHM Lyα	Skew Lyα	f_{esc} Lyα	EW Lyα [Å]	Shift Lyα	FWHM Lyα	Skew Lyα	L_B/L_R	Δv peak	Δv mom	N_{gal}
WHM	-1.42	-3.89	-3.16	-0.83	-1.87	-1.55	-2.91	-1.73	-1.28	-0.44	-1.12	-4.04	-5.24	-0.57	-1.07	-0.81	-1.17	-1.91	N:87
α/Hβ	-12.00	-4.41	-1.49	-0.12	-0.47	-8.38	-4.23	-0.23	-0.46	-0.95	-11.17	-4.04	-0.06	-0.21	-0.26	-2.69	-0.16	-0.47	N:83
I]/Hα	-8.58	-11.58	-7.69	-1.91	-3.93	-10.03	-10.45	-3.70	-4.14	-0.87	-7.19	-10.20	-2.93	-1.55	-1.73	-5.38	-1.90	-0.47	N:85
I]/Hα	-8.78	-14.63	-8.92	-2.81	-4.66	-10.30	-12.96	-2.93	-3.53	-0.82	-7.15	-13.12	-3.09	-2.37	-2.46	-6.14	-0.54	-0.15	N:85
[N2]	-8.58	-11.58	-7.69	-1.91	-3.93	-10.03	-10.45	-3.70	-4.14	-0.87	-7.19	-10.20	-2.93	-1.55	-1.73	-5.38	-1.90	-0.47	N:85
6/Hβ	-1.04	-1.06	-1.94	-0.15	-0.38	-0.84	-0.77	-0.63	-1.19	-0.15	-0.93	-1.09	-3.06	-0.38	-0.03	-0.59	-1.05	-1.16	N:85
6678	-0.29	-1.85	-1.24	-1.02	-0.44	-0.98	-2.14	-0.04	-0.53	-0.02	-0.26	-1.70	-0.10	-1.35	-0.04	-1.05	-0.03	-0.35	N:78
II/Hβ	-0.59	-0.51	-1.14	-0.80	-0.39	-0.45	-0.41	-0.24	-0.09	-0.58	-0.45	-0.34	-0.96	-1.46	-0.09	-0.27	-0.30	-0.64	N:85
I]/Hα	-2.10	-2.46	-3.45	-1.76	-0.86	-2.41	-2.50	-0.63	-1.04	-0.18	-1.63	-2.33	-2.55	-2.38	-1.84	-1.86	-0.84	-1.16	N:41
V]/Hβ	-2.14	-2.13	-5.67	-2.33	-1.34	-3.62	-4.02	-1.22	-1.66	-1.10	-1.40	-1.71	-2.41	-2.80	-1.77	-3.27	-0.63	-0.16	N:83
/[O II]	-8.99	-15.37	-8.20	-2.81	-4.42	-10.52	-13.58	-3.09	-4.33	-1.25	-7.39	-13.42	-3.40	-2.35	-2.92	-6.37	-1.12	0.22	N:86
/[O I]	-3.18	-8.56	-3.82	-0.30	-2.01	-4.77	-7.15	-1.96	-0.34	-0.22	-2.39	-8.39	-1.01	-0.24	-1.34	-3.35	-0.08	-0.14	N:50
/[O II]	-8.22	-14.35	-8.45	-2.93	-4.16	-9.45	-12.65	-3.83	-3.53	-1.22	-6.94	-12.95	-4.28	-2.50	-3.14	-5.81	-1.33	-0.48	N:86
Ar III]	-3.55	-4.98	-5.94	-2.43	-0.92	-4.20	-4.79	-2.89	-4.71	-1.37	-2.73	-4.61	-4.00	-3.96	-3.33	-3.39	-0.77	-1.14	N:43
[S II]	-1.92	-3.81	-7.04	-2.58	-1.86	-3.13	-4.23	-3.47	-3.30	-1.48	-1.22	-3.27	-3.83	-2.48	-2.87	-3.07	-1.48	-1.34	N:85
T_e	-2.27	-3.53	-5.31	-1.87	-1.58	-2.82	-3.49	-3.25	-2.40	-1.55	-1.91	-3.32	-5.61	-2.18	-2.27	-1.85	-4.44	-2.83	N:83
n_e	-2.05	-0.93	-1.61	-0.25	-0.33	-2.35	-1.44	-0.33	-0.19	-1.64	-1.56	-0.64	-0.01	-0.75	-0.60	-2.08	-0.40	-0.11	N:68
$_e / k_B$	-2.72	-2.77	-2.68	-0.75	-0.81	-2.85	-2.40	-0.46	-0.61	-0.90	-2.03	-2.26	-0.34	-1.02	-0.51	-2.13	-0.28	-0.00	N:59

Lya with stellar properties

Kendall's τ and associated *p*-value

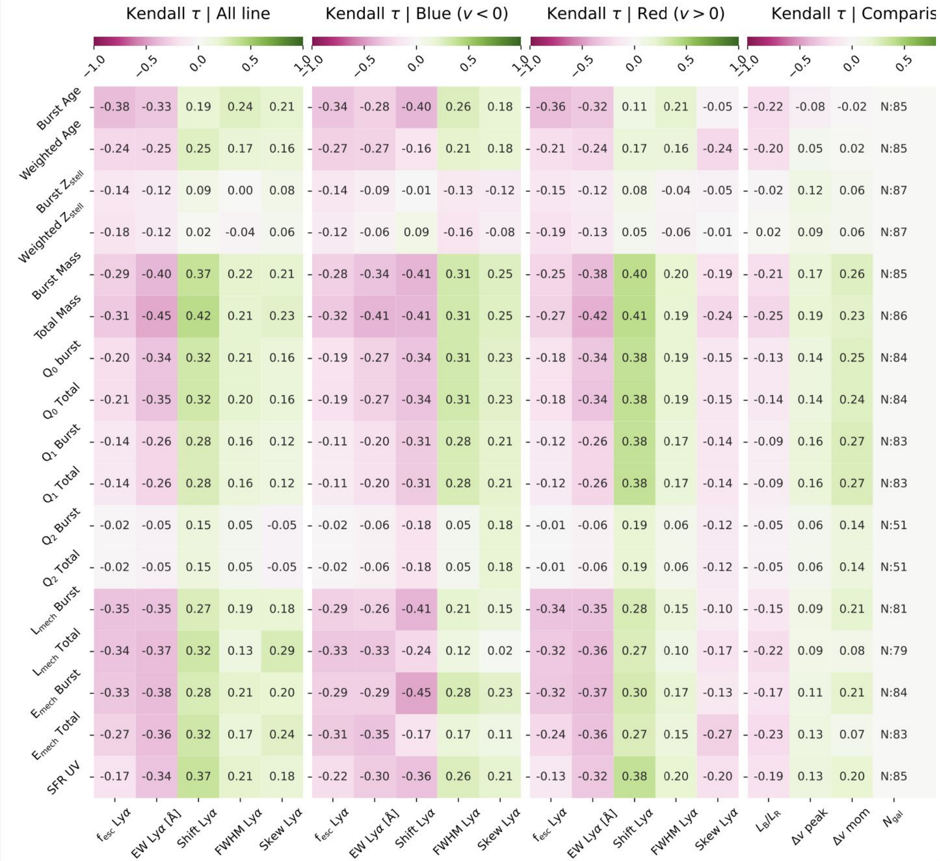

	Kendall τ | All line					Kendall τ | Blue ($v < 0$)					Kendall τ | Red ($v > 0$)					Kendall τ | Comparis			
	f_{esc} Lyα	EW Lyα [Å]	Shift Lyα	FWHM Lyα	Skew Lyα	f_{esc} Lyα	EW Lyα [Å]	Shift Lyα	FWHM Lyα	Skew Lyα	f_{esc} Lyα	EW Lyα [Å]	Shift Lyα	FWHM Lyα	Skew Lyα	L_B/L_R	Δv peak	Δv mom	N_{gal}
Burst Age	-0.38	-0.33	0.19	0.24	0.21	-0.34	-0.28	-0.40	0.26	0.18	-0.36	-0.32	0.11	0.21	-0.05	-0.22	-0.08	-0.02	N:85
Weighted Age	-0.24	-0.25	0.25	0.17	0.16	-0.27	-0.27	-0.16	0.21	0.18	-0.21	-0.24	0.17	0.16	-0.24	-0.20	0.05	0.02	N:85
Burst Z_{stell}	-0.14	-0.12	0.09	0.00	0.08	-0.14	-0.09	-0.01	-0.13	-0.12	-0.15	-0.12	0.08	-0.04	-0.05	-0.02	0.12	0.06	N:87
Weighted Z_{stell}	-0.18	-0.12	0.02	-0.04	0.06	-0.12	-0.06	0.09	-0.16	-0.08	-0.19	-0.13	0.05	-0.06	-0.01	0.02	0.09	0.06	N:87
Burst Mass	-0.29	-0.40	0.37	0.22	0.21	-0.28	-0.34	-0.41	0.31	0.25	-0.25	-0.38	0.40	0.20	-0.19	-0.21	0.17	0.26	N:85
Total Mass	-0.31	-0.45	0.42	0.21	0.23	-0.32	-0.41	-0.41	0.31	0.25	-0.27	-0.42	0.41	0.19	-0.24	-0.25	0.19	0.23	N:86
Q_0 burst	-0.20	-0.34	0.32	0.21	0.16	-0.19	-0.27	-0.34	0.31	0.23	-0.18	-0.34	0.38	0.19	-0.15	-0.13	0.14	0.25	N:84
Q_0 Total	-0.21	-0.35	0.32	0.20	0.16	-0.19	-0.27	-0.34	0.31	0.23	-0.18	-0.34	0.38	0.19	-0.15	-0.14	0.14	0.24	N:84
Q_1 Burst	-0.14	-0.26	0.28	0.16	0.12	-0.11	-0.20	-0.31	0.28	0.21	-0.12	-0.26	0.38	0.17	-0.14	-0.09	0.16	0.27	N:83
Q_1 Total	-0.14	-0.26	0.28	0.16	0.12	-0.11	-0.20	-0.31	0.28	0.21	-0.12	-0.26	0.38	0.17	-0.14	-0.09	0.16	0.27	N:83
Q_2 Burst	-0.02	-0.05	0.15	0.05	-0.05	-0.02	-0.06	-0.18	0.05	0.18	-0.01	-0.06	0.19	0.06	-0.12	-0.05	0.06	0.14	N:51
Q_2 Total	-0.02	-0.05	0.15	0.05	-0.05	-0.02	-0.06	-0.18	0.05	0.18	-0.01	-0.06	0.19	0.06	-0.12	-0.05	0.06	0.14	N:51
L_{mech} Burst	-0.35	-0.35	0.27	0.19	0.18	-0.29	-0.26	-0.41	0.21	0.15	-0.34	-0.35	0.28	0.15	-0.10	-0.15	0.09	0.21	N:81
L_{mech} Total	-0.34	-0.37	0.32	0.13	0.29	-0.33	-0.33	-0.24	0.12	0.02	-0.32	-0.36	0.27	0.10	-0.17	-0.22	0.09	0.08	N:79
E_{mech} Burst	-0.33	-0.38	0.28	0.21	0.20	-0.29	-0.29	-0.45	0.28	0.23	-0.32	-0.37	0.30	0.17	-0.13	-0.17	0.11	0.21	N:84
E_{mech} Total	-0.27	-0.36	0.32	0.17	0.24	-0.31	-0.35	-0.17	0.17	0.11	-0.24	-0.36	0.27	0.15	-0.27	-0.23	0.13	0.07	N:83
SFR UV	-0.17	-0.34	0.37	0.21	0.18	-0.22	-0.30	-0.36	0.26	0.21	-0.13	-0.32	0.38	0.20	-0.20	-0.19	0.13	0.20	N:85

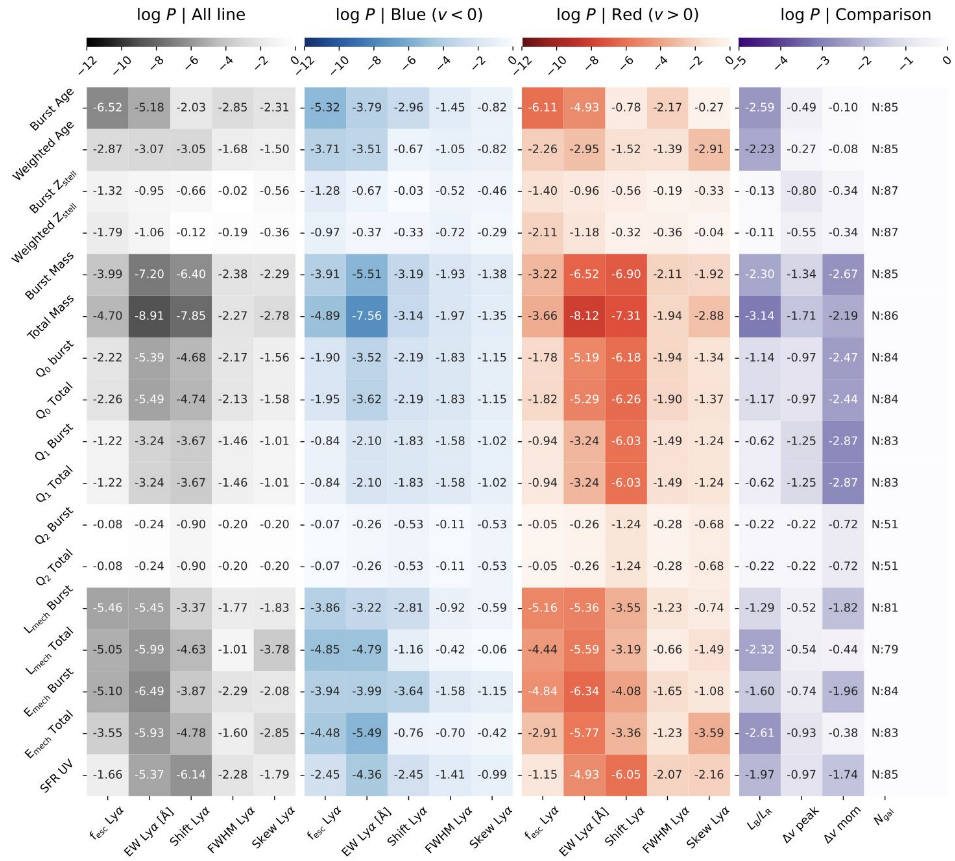

	log *P* | All line					log *P* | Blue ($v < 0$)					log *P* | Red ($v > 0$)					log *P* | Comparison			
	f_{esc} Lyα	EW Lyα [Å]	Shift Lyα	FWHM Lyα	Skew Lyα	f_{esc} Lyα	EW Lyα [Å]	Shift Lyα	FWHM Lyα	Skew Lyα	f_{esc} Lyα	EW Lyα [Å]	Shift Lyα	FWHM Lyα	Skew Lyα	L_B/L_R	Δv peak	Δv mom	N_{gal}
Burst Age	-6.52	-5.18	-2.03	-2.85	-2.31	-5.32	-3.79	-2.96	-1.45	-0.82	-6.11	-4.93	-0.78	-2.17	-0.27	-2.59	-0.49	-0.10	N:85
Weighted Age	-2.87	-3.07	-3.05	-1.68	-1.50	-3.71	-3.51	-0.67	-1.05	-0.82	-2.26	-2.95	-1.52	-1.39	-2.91	-2.23	-0.27	-0.08	N:85
Burst Z_{stell}	-1.32	-0.95	-0.66	-0.02	-0.56	-1.28	-0.67	-0.03	-0.52	-0.46	-1.40	-0.96	-0.56	-0.19	-0.33	-0.13	-0.80	-0.34	N:87
Weighted Z_{stell}	-1.79	-1.06	-0.12	-0.19	-0.36	-0.97	-0.37	-0.33	-0.72	-0.29	-2.11	-1.18	-0.32	-0.36	-0.04	-0.11	-0.55	-0.34	N:87
Burst Mass	-3.99	-7.20	-6.40	-2.38	-2.29	-3.91	-5.51	-3.19	-1.93	-1.38	-3.22	-6.52	-6.90	-2.11	-1.92	-2.30	-1.34	-2.67	N:85
Total Mass	-4.70	-8.91	-7.85	-2.27	-2.78	-4.89	-7.56	-3.14	-1.97	-1.35	-3.66	-8.12	-7.31	-1.94	-2.88	-3.14	-1.71	-2.19	N:86
Q_0 burst	-2.22	-5.39	-4.68	-2.17	-1.56	-1.90	-3.52	-2.19	-1.83	-1.15	-1.78	-5.19	-6.18	-1.94	-1.34	-1.14	-0.97	-2.47	N:84
Q_0 Total	-2.26	-5.49	-4.74	-2.13	-1.58	-1.95	-3.62	-2.19	-1.83	-1.15	-1.82	-5.29	-6.26	-1.90	-1.37	-1.17	-0.97	-2.44	N:84
Q_1 Burst	-1.22	-3.24	-3.67	-1.46	-1.01	-0.84	-2.10	-1.83	-1.58	-1.02	-0.94	-3.24	-6.03	-1.49	-1.24	-0.62	-1.25	-2.87	N:83
Q_1 Total	-1.22	-3.24	-3.67	-1.46	-1.01	-0.84	-2.10	-1.83	-1.58	-1.02	-0.94	-3.24	-6.03	-1.49	-1.24	-0.62	-1.25	-2.87	N:83
Q_2 Burst	-0.08	-0.24	-0.90	-0.20	-0.20	-0.07	-0.26	-0.53	-0.11	-0.53	-0.05	-0.26	-1.24	-0.28	-0.68	-0.22	-0.22	-0.72	N:51
Q_2 Total	-0.08	-0.24	-0.90	-0.20	-0.20	-0.07	-0.26	-0.53	-0.11	-0.53	-0.05	-0.26	-1.24	-0.28	-0.68	-0.22	-0.22	-0.72	N:51
L_{mech} Burst	-5.46	-5.45	-3.37	-1.77	-1.83	-3.86	-3.22	-2.81	-0.92	-0.59	-5.16	-5.36	-3.55	-1.23	-0.74	-1.29	-0.52	-1.82	N:81
L_{mech} Total	-5.05	-5.99	-4.63	-1.01	-3.78	-4.85	-4.79	-1.16	-0.42	-0.06	-4.44	-5.59	-3.19	-0.66	-1.49	-2.32	-0.54	-0.44	N:79
E_{mech} Burst	-5.10	-6.49	-3.87	-2.29	-2.08	-3.94	-3.99	-3.64	-1.58	-1.15	-4.84	-6.34	-4.08	-1.65	-1.08	-1.60	-0.74	-1.96	N:84
E_{mech} Total	-3.55	-5.93	-4.78	-1.60	-2.85	-4.48	-5.49	-0.76	-0.70	-0.42	-2.91	-5.77	-3.36	-1.23	-3.59	-2.61	-0.93	-0.38	N:83
SFR UV	-1.66	-5.37	-6.14	-2.28	-1.79	-2.45	-4.36	-2.45	-1.41	-0.99	-1.15	-4.93	-6.05	-2.07	-2.16	-1.97	-0.97	-1.74	N:85

Lya with mixed nebular and stellar properties

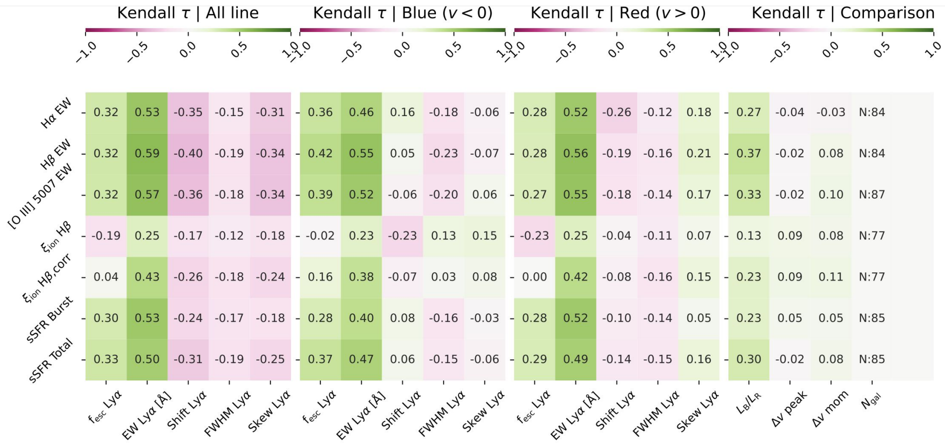

	Kendall τ | All line					Kendall τ | Blue ($v<0$)					Kendall τ | Red ($v>0$)					Kendall τ | Comparison			
	f_{esc} Lyα	EW Lyα [Å]	Shift Lyα	FWHM Lyα	Skew Lyα	f_{esc} Lyα	EW Lyα [Å]	Shift Lyα	FWHM Lyα	Skew Lyα	f_{esc} Lyα	EW Lyα [Å]	Shift Lyα	FWHM Lyα	Skew Lyα	L_B/L_R	Δv peak	Δv mom	N_{gal}
Hα EW	0.32	0.53	-0.35	-0.15	-0.31	0.36	0.46	0.16	-0.18	-0.06	0.28	0.52	-0.26	-0.12	0.18	0.27	-0.04	-0.03	N:84
Hβ EW	0.32	0.59	-0.40	-0.19	-0.34	0.42	0.55	0.05	-0.23	-0.07	0.28	0.56	-0.19	-0.16	0.21	0.37	-0.02	0.08	N:84
[O III] 5007 EW	0.32	0.57	-0.36	-0.18	-0.34	0.39	0.52	-0.06	-0.20	0.06	0.27	0.55	-0.18	-0.14	0.17	0.33	-0.02	0.10	N:87
ξ_{ion} Hβ	-0.19	0.25	-0.17	-0.12	-0.18	-0.02	0.23	-0.23	0.13	0.15	-0.23	0.25	-0.04	-0.11	0.07	0.13	0.09	0.08	N:77
ξ_{ion} Hβ,corr	0.04	0.43	-0.26	-0.18	-0.24	0.16	0.38	-0.07	0.03	0.08	0.00	0.42	-0.08	-0.16	0.15	0.23	0.09	0.11	N:77
sSFR Burst	0.30	0.53	-0.24	-0.17	-0.18	0.28	0.40	0.08	-0.16	-0.03	0.28	0.52	-0.10	-0.14	0.05	0.23	0.05	0.05	N:85
sSFR Total	0.33	0.50	-0.31	-0.19	-0.25	0.37	0.47	0.06	-0.15	-0.06	0.29	0.49	-0.14	-0.15	0.16	0.30	-0.02	0.08	N:85

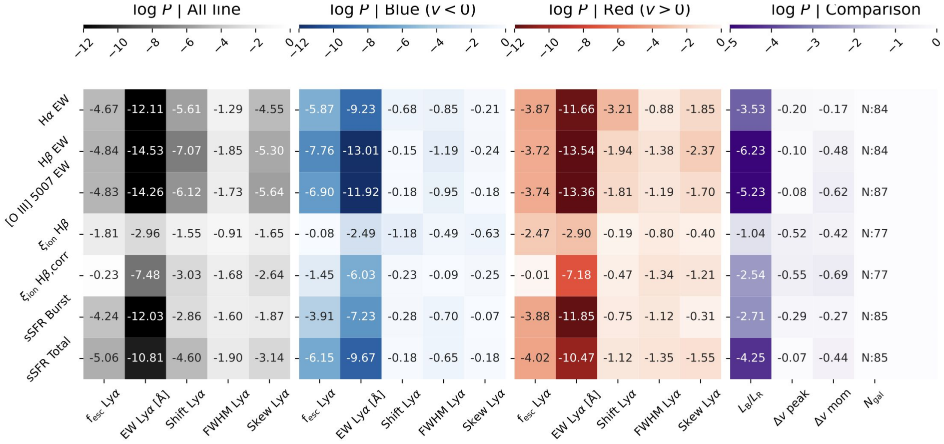

	log P | All line					log P | Blue ($v<0$)					log P | Red ($v>0$)					log P | Comparison			
	f_{esc} Lyα	EW Lyα [Å]	Shift Lyα	FWHM Lyα	Skew Lyα	f_{esc} Lyα	EW Lyα [Å]	Shift Lyα	FWHM Lyα	Skew Lyα	f_{esc} Lyα	EW Lyα [Å]	Shift Lyα	FWHM Lyα	Skew Lyα	L_B/L_R	Δv peak	Δv mom	N_{gal}
Hα EW	-4.67	-12.11	-5.61	-1.29	-4.55	-5.87	-9.23	-0.68	-0.85	-0.21	-3.87	-11.66	-3.21	-0.88	-1.85	-3.53	-0.20	-0.17	N:84
Hβ EW	-4.84	-14.53	-7.07	-1.85	-5.30	-7.76	-13.01	-0.15	-1.19	-0.24	-3.72	-13.54	-1.94	-1.38	-2.37	-6.23	-0.10	-0.48	N:84
[O III] 5007 EW	-4.83	-14.26	-6.12	-1.73	-5.64	-6.90	-11.92	-0.18	-0.95	-0.18	-3.74	-13.36	-1.81	-1.19	-1.70	-5.23	-0.08	-0.62	N:87
ξ_{ion} Hβ	-1.81	-2.96	-1.55	-0.91	-1.65	-0.08	-2.49	-1.18	-0.49	-0.63	-2.47	-2.90	-0.19	-0.80	-0.40	-1.04	-0.52	-0.42	N:77
ξ_{ion} Hβ,corr	-0.23	-7.48	-3.03	-1.68	-2.64	-1.45	-6.03	-0.23	-0.09	-0.25	-0.01	-7.18	-0.47	-1.34	-1.21	-2.54	-0.55	-0.69	N:77
sSFR Burst	-4.24	-12.03	-2.86	-1.60	-1.87	-3.91	-7.23	-0.28	-0.70	-0.07	-3.88	-11.85	-0.75	-1.12	-0.31	-2.71	-0.29	-0.27	N:85
sSFR Total	-5.06	-10.81	-4.60	-1.90	-3.14	-6.15	-9.67	-0.18	-0.65	-0.18	-4.02	-10.47	-1.12	-1.35	-1.55	-4.25	-0.07	-0.44	N:85

I.e. we have one set of these plots for every measured quantity

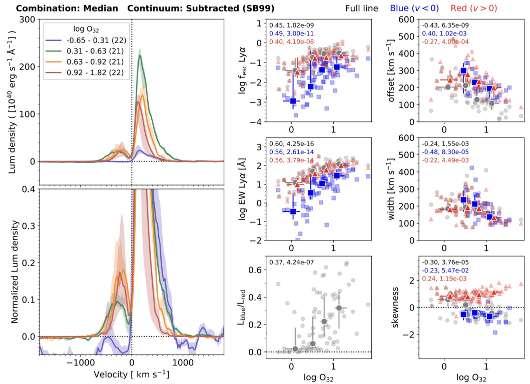

A coherent picture

Lyα equivalent width of local galaxies scales strongly with

- (i.) nebular metallicity: lower O/H → more Lyα
- (ii.) ionization parameter: higher log U → more Lyα
- (iii.) age of starburst: younger → more Lyα

All expected from Lyα production standpoint

⇒ This looks like an evolutionary sequence with stars

However: **Lyα escape fraction** and $\mathbf{L_{blue}/L_{red}}$ change similarly

- (i.) **Blueshifted emission evolves faster than red**
- (ii.) Dust not as relevant as **O/H** or ***U***
- (iii.) Absorption lines get weaker in lockstep

Nothing to do with production
All in the transfer

⇒ probably related to photoionization feedback, or the very first supernovae

Objectives and contents

- **Study of low-redshift Lya emitters**
    - Sample overview
    - Lya output with properties of stars & gas
    - Evolution & acceleration of galaxy winds
- **Evolution of profiles with redshift**
    - Intrinsic LAE profiles do not evolve significantly
    - IGM is responsible for reshaping Lya
- **Lya profiles to infer IGM properties during the EoR**
    - Derive sizes of ionized regions
    - Estimate the LyC escape fraction

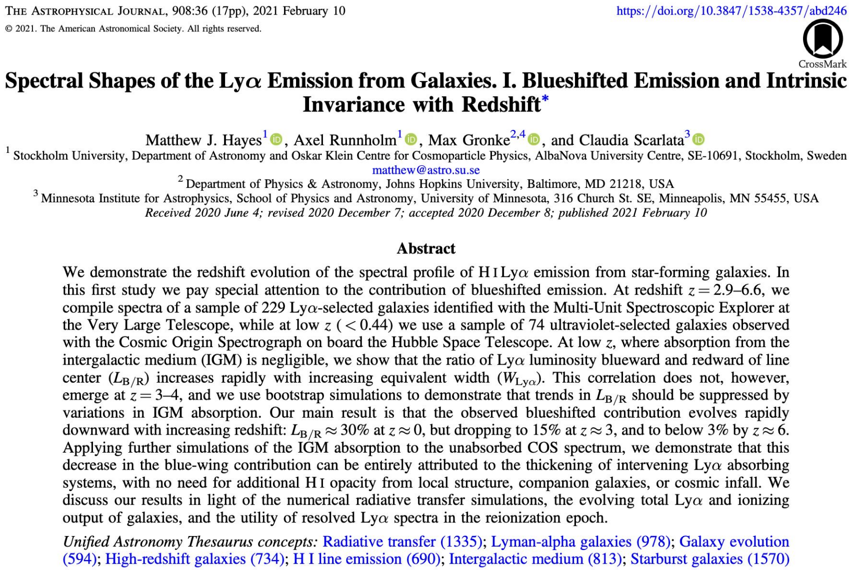

The Astrophysical Journal, 908:36 (17pp), 2021 February 10 https://doi.org/10.3847/1538-4357/abd246

CrossMark

Spectral Shapes of the Lyα Emission from Galaxies. I. Blueshifted Emission and Intrinsic Invariance with Redshift*

Matthew J. Hayes[1], Axel Runnholm[1], Max Gronke[2,4], and Claudia Scarlata[3]
[1] Stockholm University, Department of Astronomy and Oskar Klein Centre for Cosmoparticle Physics, AlbaNova University Centre, SE-10691, Stockholm, Sweden
matthew@astro.su.se
[2] Department of Physics & Astronomy, Johns Hopkins University, Baltimore, MD 21218, USA
[3] Minnesota Institute for Astrophysics, School of Physics and Astronomy, University of Minnesota, 316 Church St. SE, Minneapolis, MN 55455, USA

Received 2020 June 4; revised 2020 December 7; accepted 2020 December 8; published 2021 February 10

Abstract

We demonstrate the redshift evolution of the spectral profile of H I Lyα emission from star-forming galaxies. In this first study we pay special attention to the contribution of blueshifted emission. At redshift $z = 2.9$–6.6, we compile spectra of a sample of 229 Lyα-selected galaxies identified with the Multi-Unit Spectroscopic Explorer at the Very Large Telescope, while at low z (< 0.44) we use a sample of 74 ultraviolet-selected galaxies observed with the Cosmic Origin Spectrograph on board the Hubble Space Telescope. At low z, where absorption from the intergalactic medium (IGM) is negligible, we show that the ratio of Lyα luminosity blueward and redward of line center ($L_{\mathrm{B/R}}$) increases rapidly with increasing equivalent width ($W_{\mathrm{Ly}\alpha}$). This correlation does not, however, emerge at $z = 3$–4, and we use bootstrap simulations to demonstrate that trends in $L_{\mathrm{B/R}}$ should be suppressed by variations in IGM absorption. Our main result is that the observed blueshifted contribution evolves rapidly downward with increasing redshift: $L_{\mathrm{B/R}} \approx 30\%$ at $z \approx 0$, but dropping to 15% at $z \approx 3$, and to below 3% by $z \approx 6$. Applying further simulations of the IGM absorption to the unabsorbed COS spectrum, we demonstrate that this decrease in the blue-wing contribution can be entirely attributed to the thickening of intervening Lyα absorbing systems, with no need for additional H I opacity from local structure, companion galaxies, or cosmic infall. We discuss our results in light of the numerical radiative transfer simulations, the evolving total Lyα and ionizing output of galaxies, and the utility of resolved Lyα spectra in the reionization epoch.

Unified Astronomy Thesaurus concepts: Radiative transfer (1335); Lyman-alpha galaxies (978); Galaxy evolution (594); High-redshift galaxies (734); H I line emission (690); Intergalactic medium (813); Starburst galaxies (1570)

Hayes et al 2021
ApJ, 908, 36

Comparison of Lya emitter profiles with high-z

MUSE-WIDE

Urrutia+2019; Herenz+2017

479 Lya emitters at z=2.9 - 6.6

Publicly available from
https://musewide.aip.de/project/

CANDELS Deep in GOODS-S
→ best HST data available

Focus on the ratio L_{blue}/L_{red}

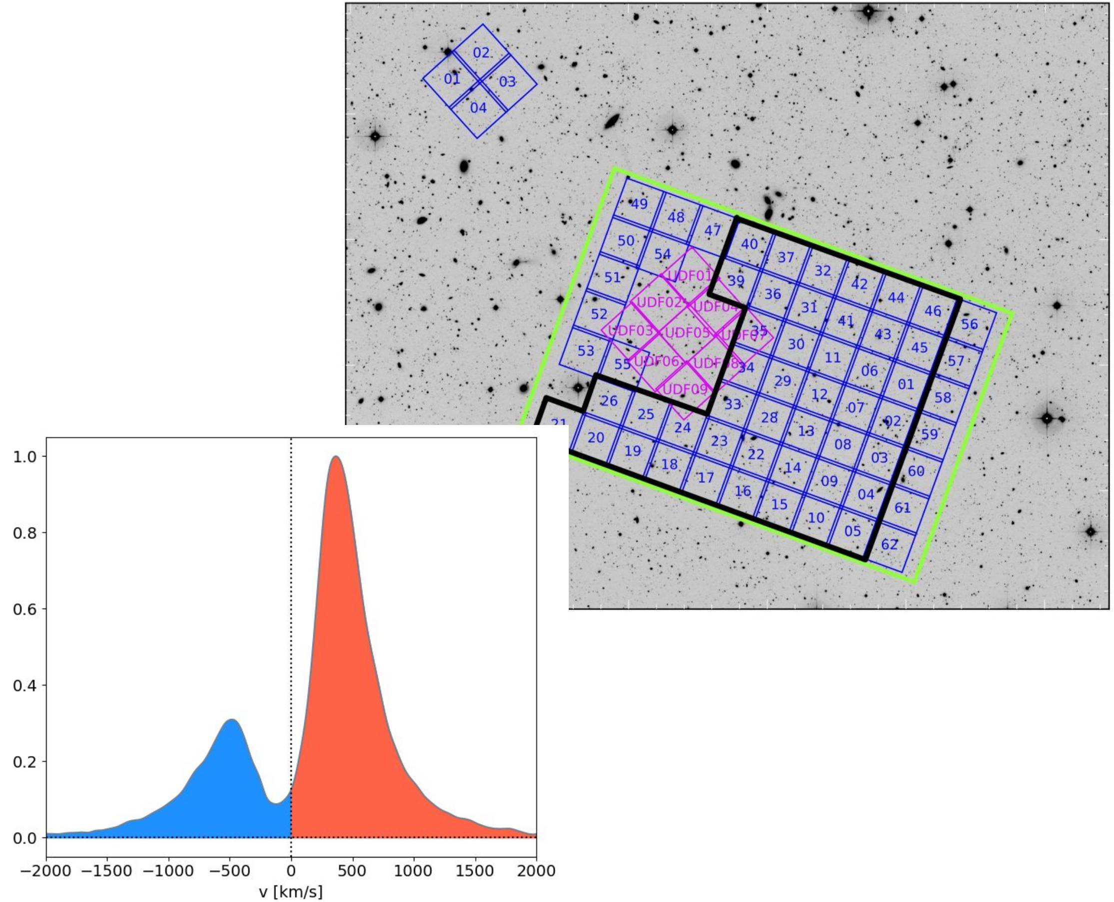

Evolution of Lya-emitter profiles

87 low-z sources

479 sources at z=3 – 6.6

Match the COS and MUSE samples in Lya luminosity range and EW

Focus on the ratio L_{blue}/L_{red}

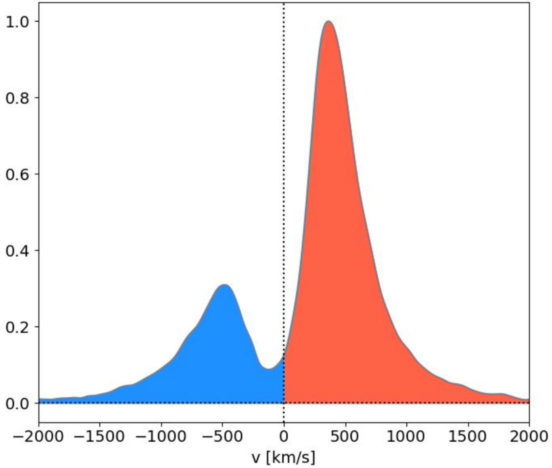

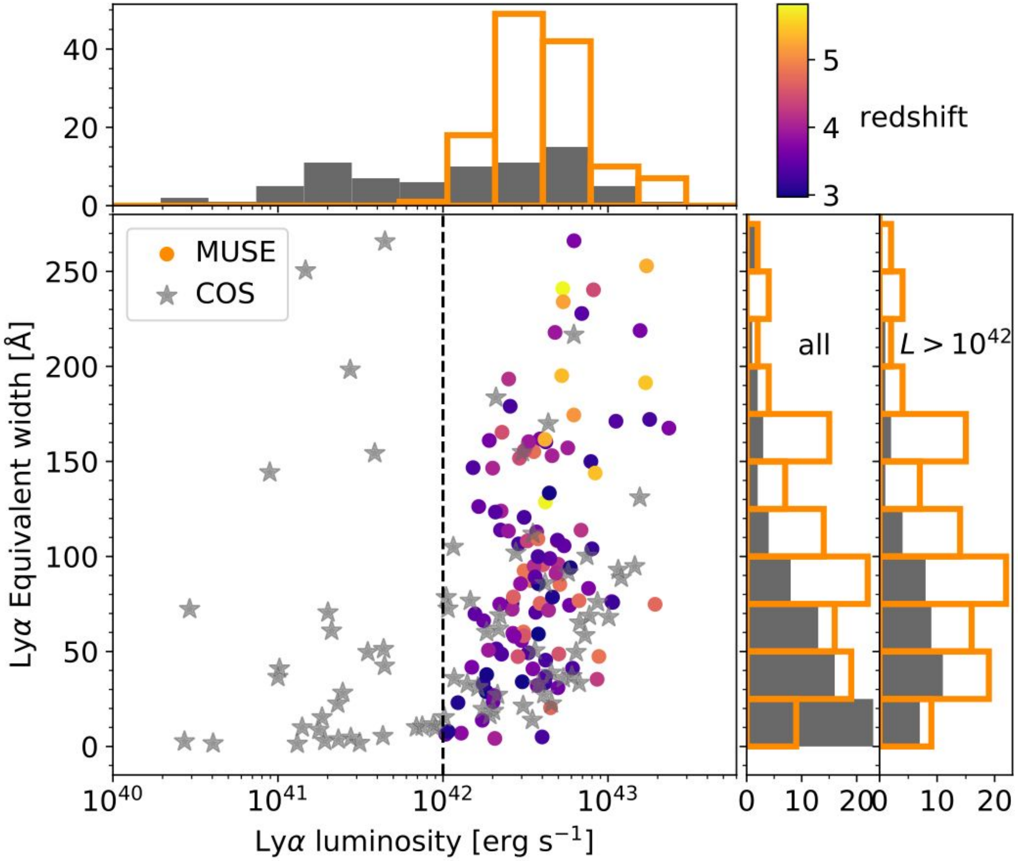

Evolution of Lya-emitter profiles

Normalize & stack the Lya profiles in bins of different redshift

Lya L_{blue}/L_{red} goes from:

- 0.32 at z=0.2
- 0.17 at z=3.2
- 0.16 at z=3.6
- 0.08 at z=4.0
- 0.10 at z=4.5
- 0.02 at z=5.2

If the galaxies are changing, they are doing so in a very conspicuous way…

C.f. quasar spectra!

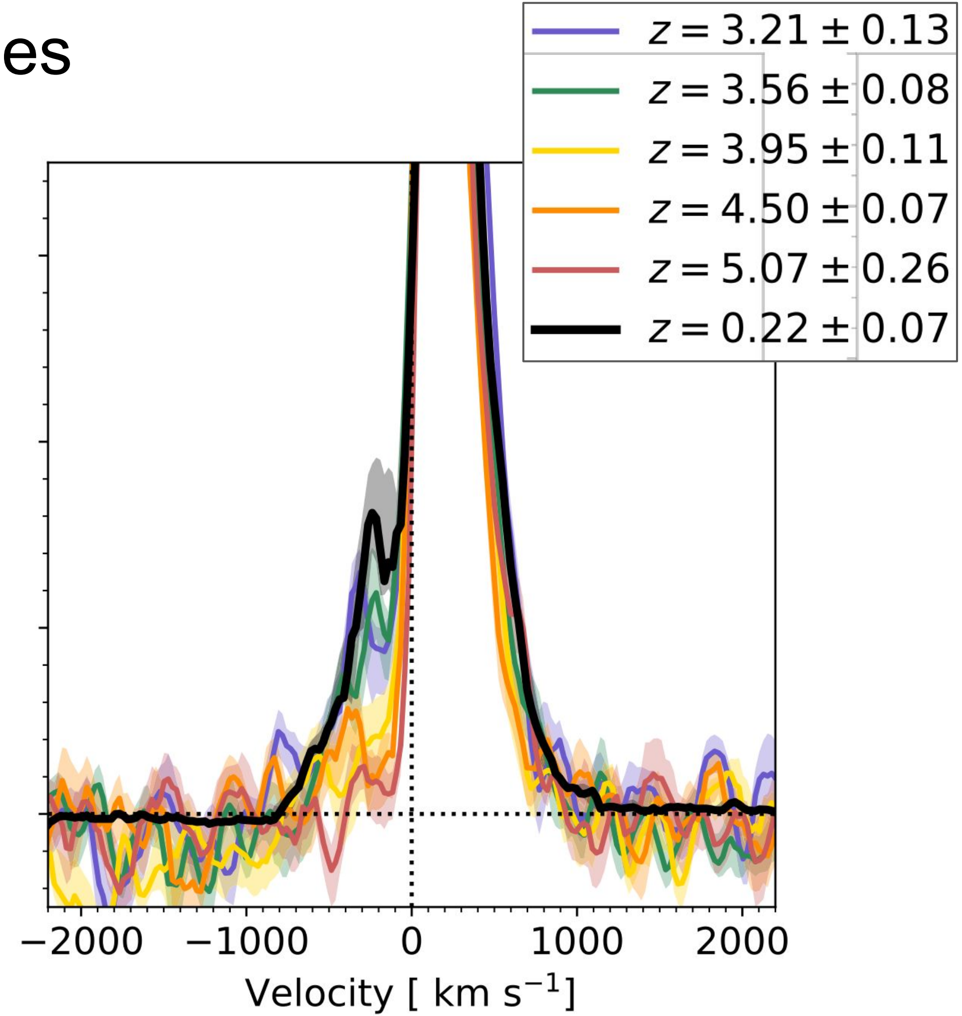

Evolution of Lya-emitter profiles

Normalize & stack the Lya profiles in bins of different redshift

Lya L_{blue}/L_{red} goes from:

0.32 at z=0.2

0.17 at z=3.2

0.16 at z=3.6

0.08 at z=4.0

0.10 at z=4.5

0.02 at z=5.2

0.26 at z=2.2

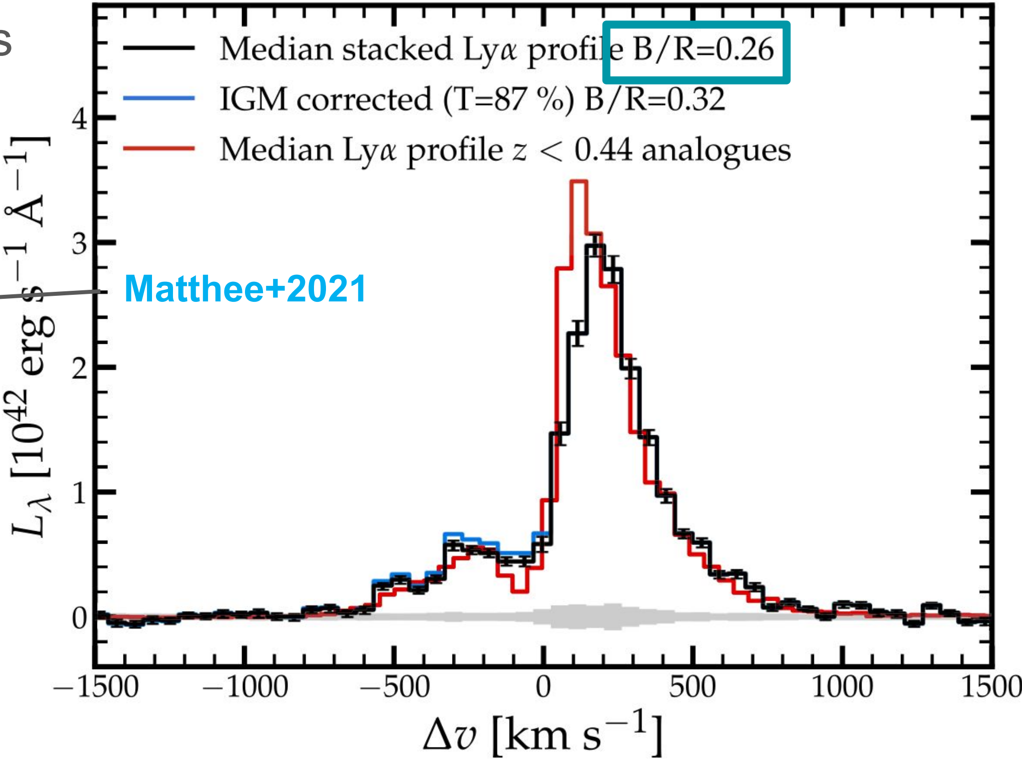

If the galaxies are changing, they are doing so in a very conspicuous way…

C.f. quasar spectra!

Evolution of the IGM opacity

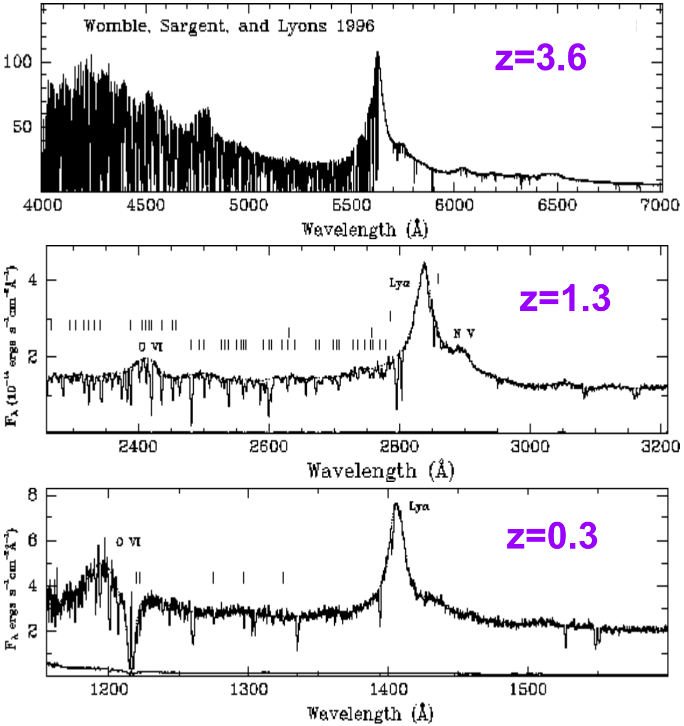

Increasing redshift

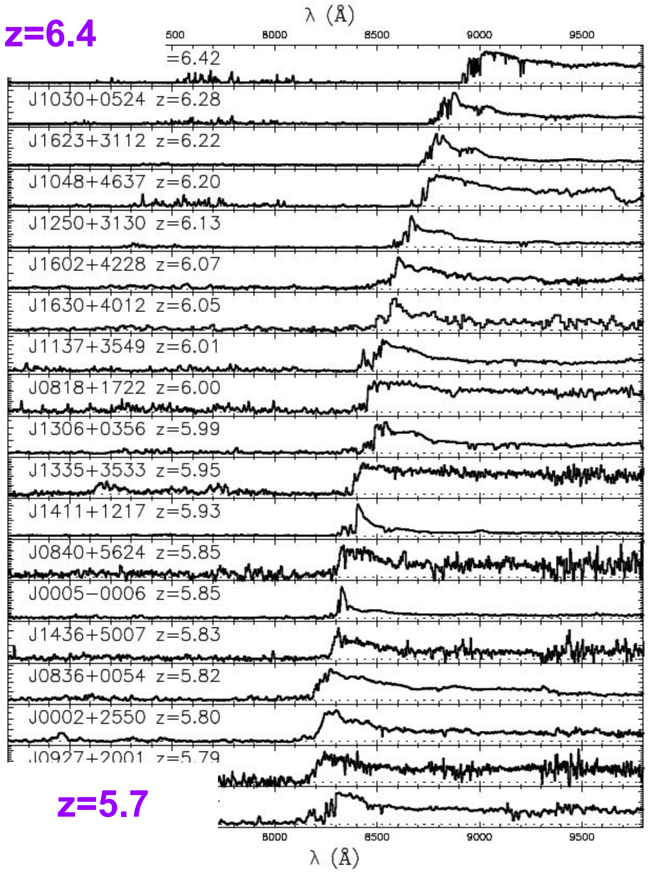

The multivariate distribution functions **$d^3N / dN_{HI}, db, dz$**

All are well known from quasar observations

Evolution of the IGM opacity

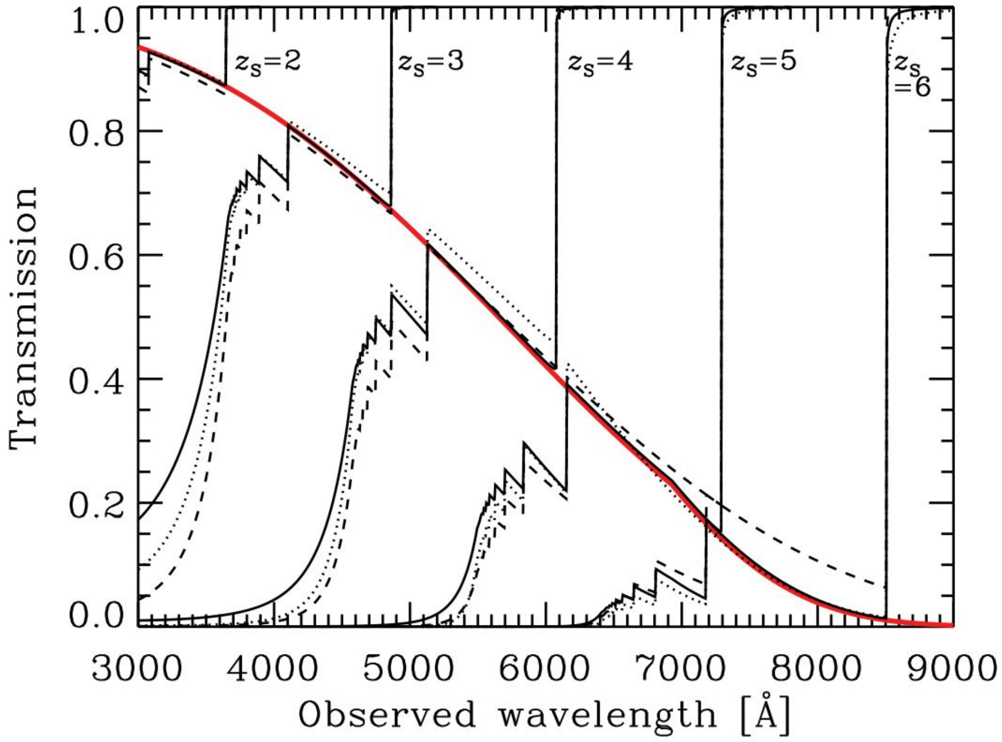

Inoue & Iwata (2008); Inoue+2014 publish set of PDFs to implement this (others are available)

Evolution of Lya-emitter profiles

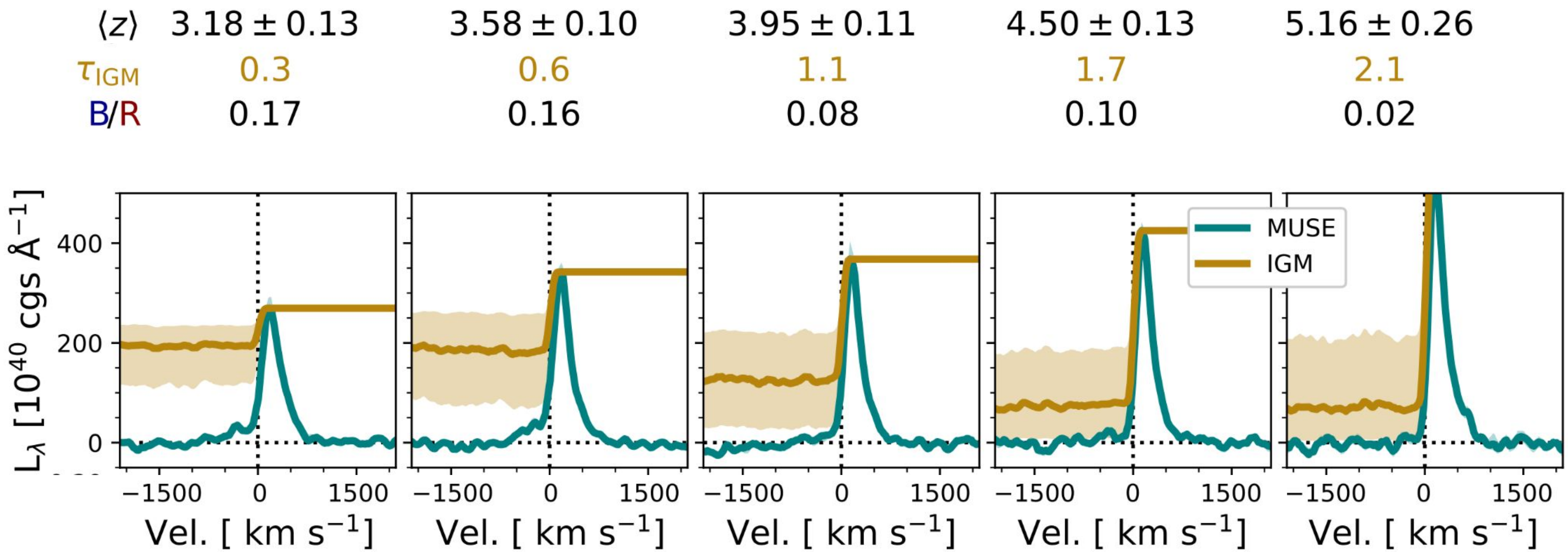

$\langle z \rangle$	3.18 ± 0.13	3.58 ± 0.10	3.95 ± 0.11	4.50 ± 0.13	5.16 ± 0.26
τ_{IGM}	0.3	0.6	1.1	1.7	2.1
B/R	0.17	0.16	0.08	0.10	0.02

Lya opacity increases across with redshift

Evolution of Lya-emitter profiles

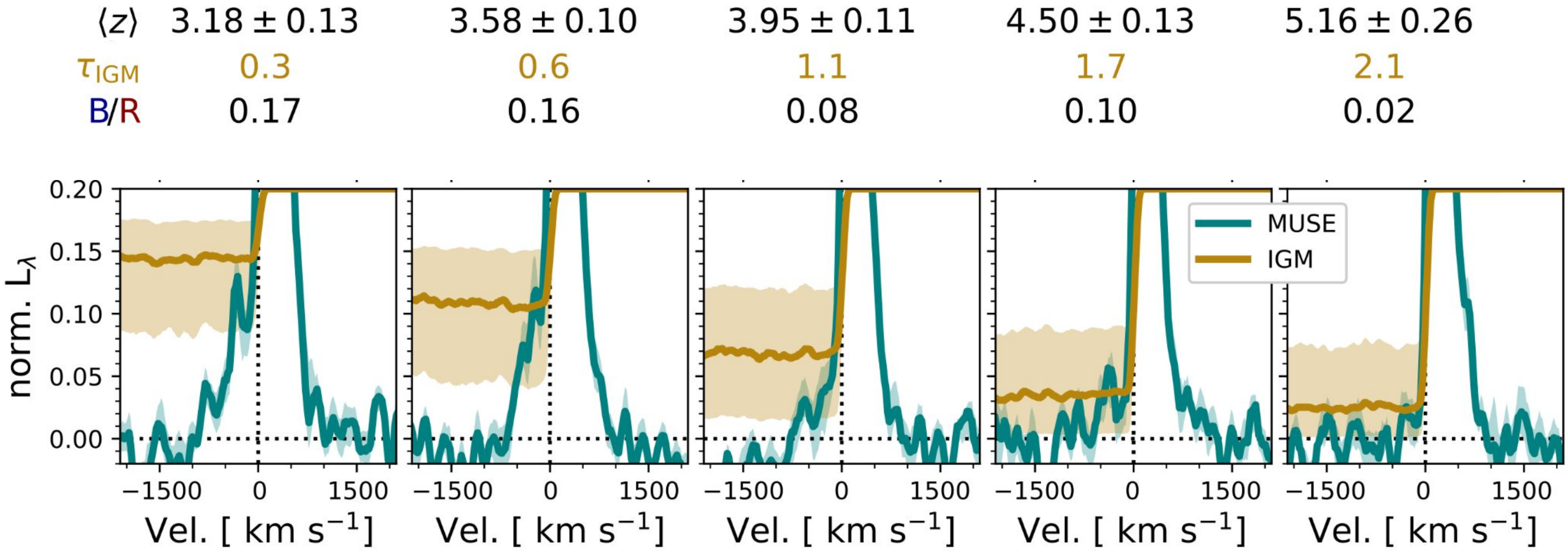

Lya opacity increase appears to match decrease in blueshifted emission

Evolution of Lya-emitter profiles

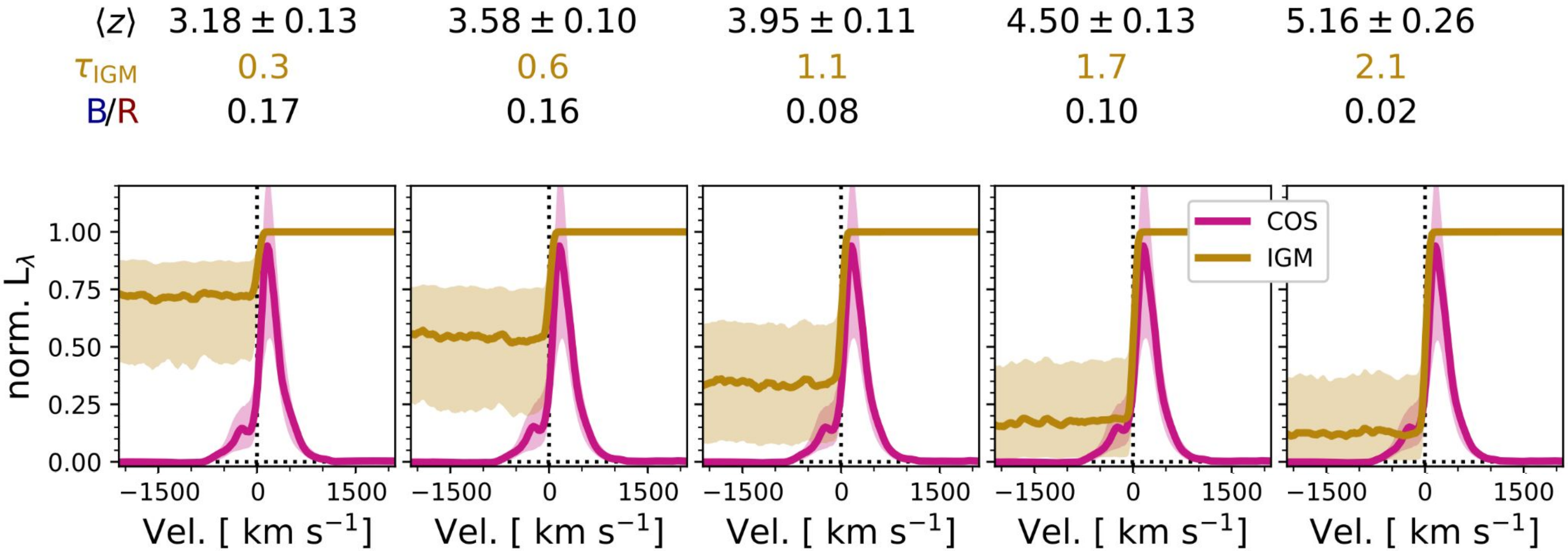

$\langle z \rangle$	3.18 ± 0.13	3.58 ± 0.10	3.95 ± 0.11	4.50 ± 0.13	5.16 ± 0.26
τ_{IGM}	0.3	0.6	1.1	1.7	2.1
B/R	0.17	0.16	0.08	0.10	0.02

How would the COS profile look if it were absorbed by this opacity?

Evolution of Lya-emitter profiles

$\langle z \rangle$	3.18 ± 0.13	3.58 ± 0.10	3.95 ± 0.11	4.50 ± 0.13	5.16 ± 0.26
τ_{IGM}	0.3	0.6	1.1	1.7	2.1
B/R	0.17	0.16	0.08	0.10	0.02

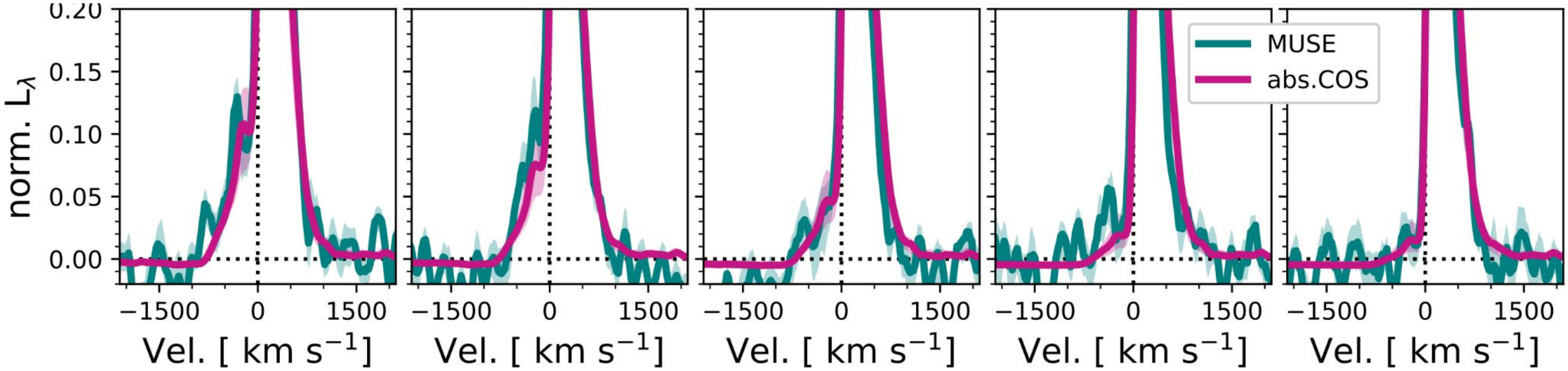

The absorbed COS profile looks exactly like the observed profiles at z=3-6!

We cannot detect redshift evolution of Lya spectral profiles

Intrinsic Lya properties do not change with redshift

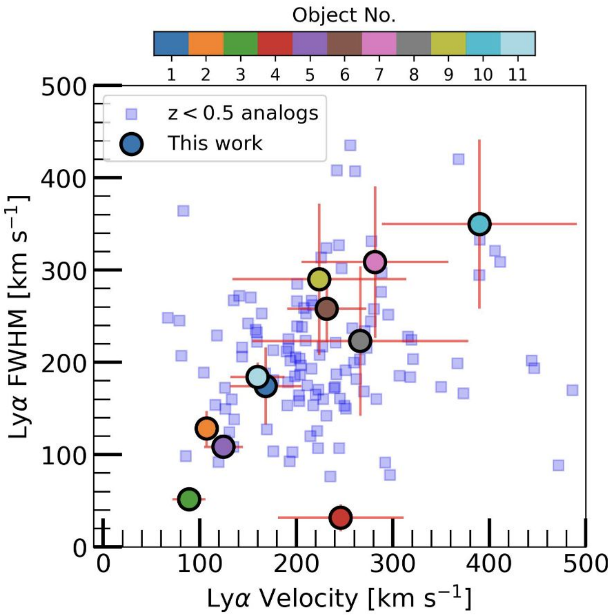

Agreement from recent JWST obs

Roy+2023

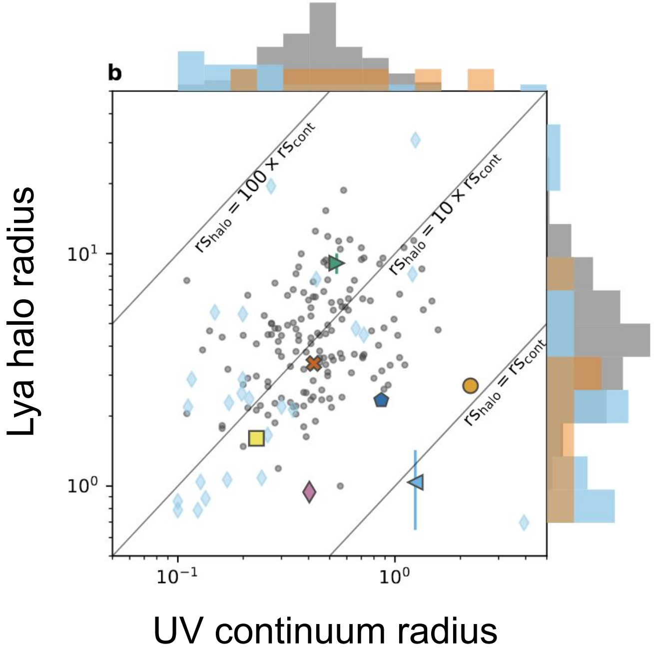

Lya halos at high-z resemble those at low-z

Runnholm+2023; Rasekh+2022

Can happily apply low-z Lya profiles to high-z galaxies

Objectives and contents

- **Study of low-redshift Lya emitters**
  - Sample overview
  - Lya output with properties of stars & gas
  - Evolution & acceleration of galaxy winds
- **Evolution of profiles with redshift**
  - Intrinsic LAE spectra do not evolve signific
  - IGM is responsible for reshaping Lya
- **Lya profiles to infer IGM properties during the EoR**
  - Derive sizes of ionized regions
  - Estimate the LyC escape fraction

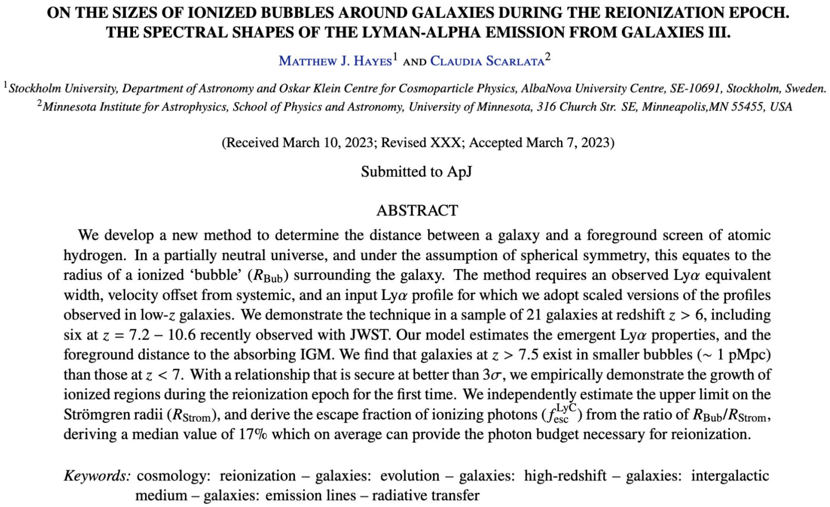

ON THE SIZES OF IONIZED BUBBLES AROUND GALAXIES DURING THE REIONIZATION EPOCH.
THE SPECTRAL SHAPES OF THE LYMAN-ALPHA EMISSION FROM GALAXIES III.

Matthew J. Hayes[1] and Claudia Scarlata[2]

[1] *Stockholm University, Department of Astronomy and Oskar Klein Centre for Cosmoparticle Physics, AlbaNova University Centre, SE-10691, Stockholm, Sweden.*
[2] *Minnesota Institute for Astrophysics, School of Physics and Astronomy, University of Minnesota, 316 Church Str. SE, Minneapolis,MN 55455, USA*

(Received March 10, 2023; Revised XXX; Accepted March 7, 2023)

Submitted to ApJ

ABSTRACT

We develop a new method to determine the distance between a galaxy and a foreground screen of atomic hydrogen. In a partially neutral universe, and under the assumption of spherical symmetry, this equates to the radius of a ionized 'bubble' ($R_{\rm Bub}$) surrounding the galaxy. The method requires an observed Lyα equivalent width, velocity offset from systemic, and an input Lyα profile for which we adopt scaled versions of the profiles observed in low-z galaxies. We demonstrate the technique in a sample of 21 galaxies at redshift $z > 6$, including six at $z = 7.2 - 10.6$ recently observed with JWST. Our model estimates the emergent Lyα properties, and the foreground distance to the absorbing IGM. We find that galaxies at $z > 7.5$ exist in smaller bubbles ($\sim$ 1 pMpc) than those at $z < 7$. With a relationship that is secure at better than 3σ, we empirically demonstrate the growth of ionized regions during the reionization epoch for the first time. We independently estimate the upper limit on the Strömgren radii ($R_{\rm Strom}$), and derive the escape fraction of ionizing photons ($f_{\rm esc}^{\rm LyC}$) from the ratio of $R_{\rm Bub}/R_{\rm Strom}$, deriving a median value of 17% which on average can provide the photon budget necessary for reionization.

Keywords: cosmology: reionization – galaxies: evolution – galaxies: high-redshift – galaxies: intergalactic medium – galaxies: emission lines – radiative transfer

Hayes & Scarlata 2023
arXiv:2303.03160

How the IGM affects Lya

1. Absorbs all blueshifted emission
2. Damping wing reduces redshifted flux and shifts moment to higher velocities

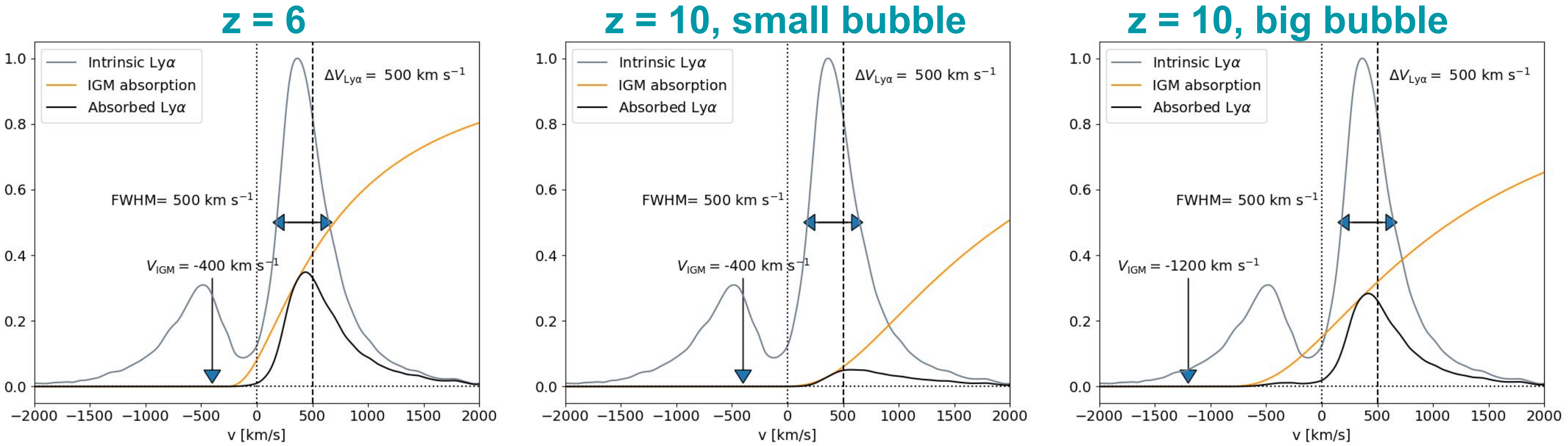

Know the intrinsic line profile?

Estimate intrinsic EW and velocity offset of IGM

Into the Reionization Epoch

- 23 known galaxies at $z = 6\text{-}11$ with z_{sys} [Δv(Lya)], *EW*(Lya), ανδ M_{UV}
  Endsley+2022, Tang+2023, Bunker+2023, Saxena+2023, Jung+2023
- Lya profiles do not evolve significantly with redshift + we can predict them
  Hayes+2021, Hayes+2023
- Similar nebular conditions in low & high z analogs
  Cameron+2023, Schaerer+2023, Brinchmann+2023
- *EW*(Lya) distributions known to z~6 ⇒ prior from M_{UV}
  Hashimoto+2018 and many others…

Hierarchical inference model to get intrinsic V_{igm}

Hayes & Scarlata 2023

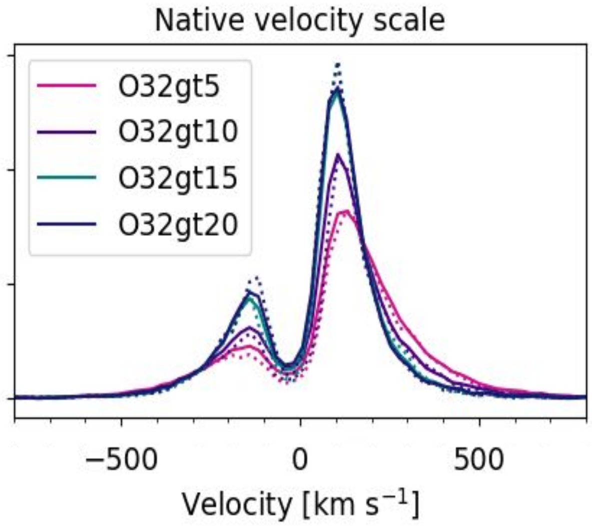

Native velocity scale

Example with GNz11 at z=10.6

z_{sys} = 10.6 Δ*v*(Lya) = 555 km/s *EW*(Lya) = 18 Å M_{UV}= -21.5

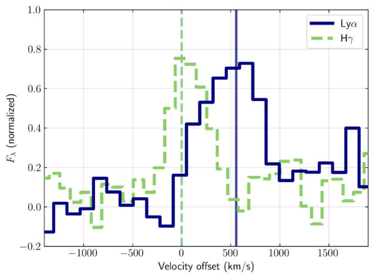

Bunker+2023

EW_0 = 171 Å
(150-370) Å

v_{IGM} = -714 km/s
(450-990) km/s

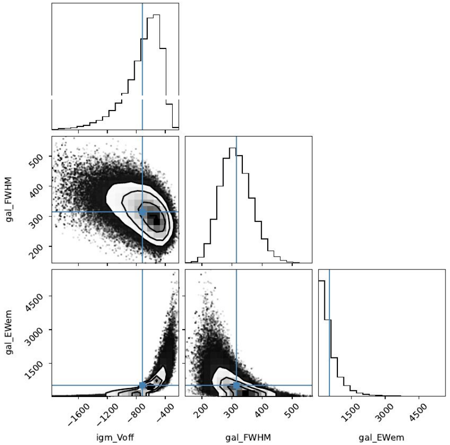

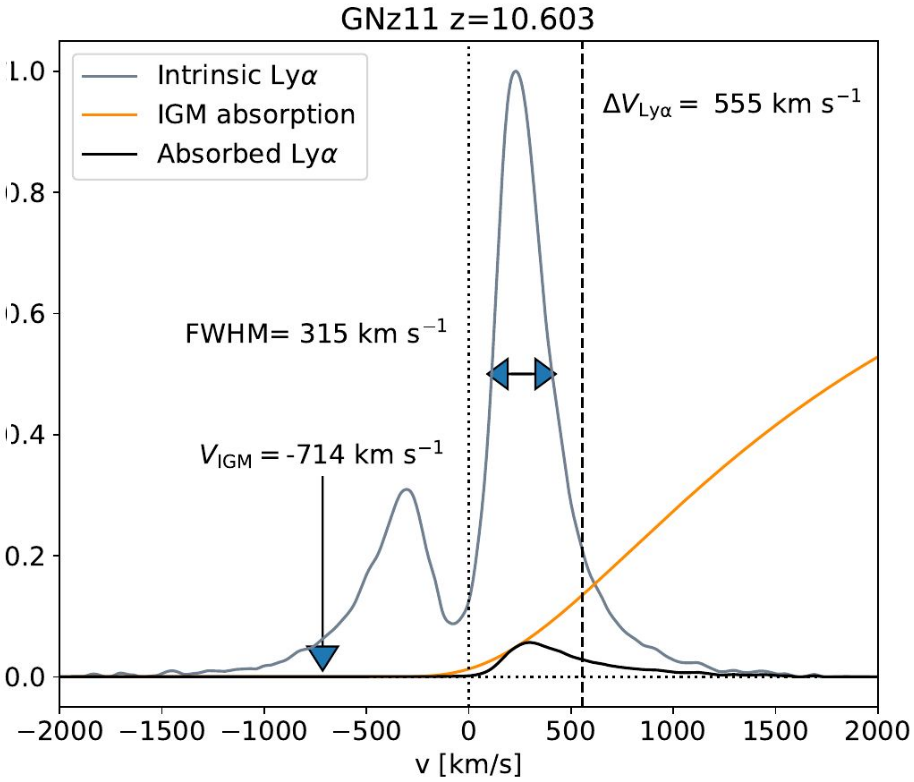

Bubble Size Distribution at z = 6 - 11

HII regions: **smaller at higher z**

N = 23 Κενδαλλ τ = -0.34 *p* = 0.02

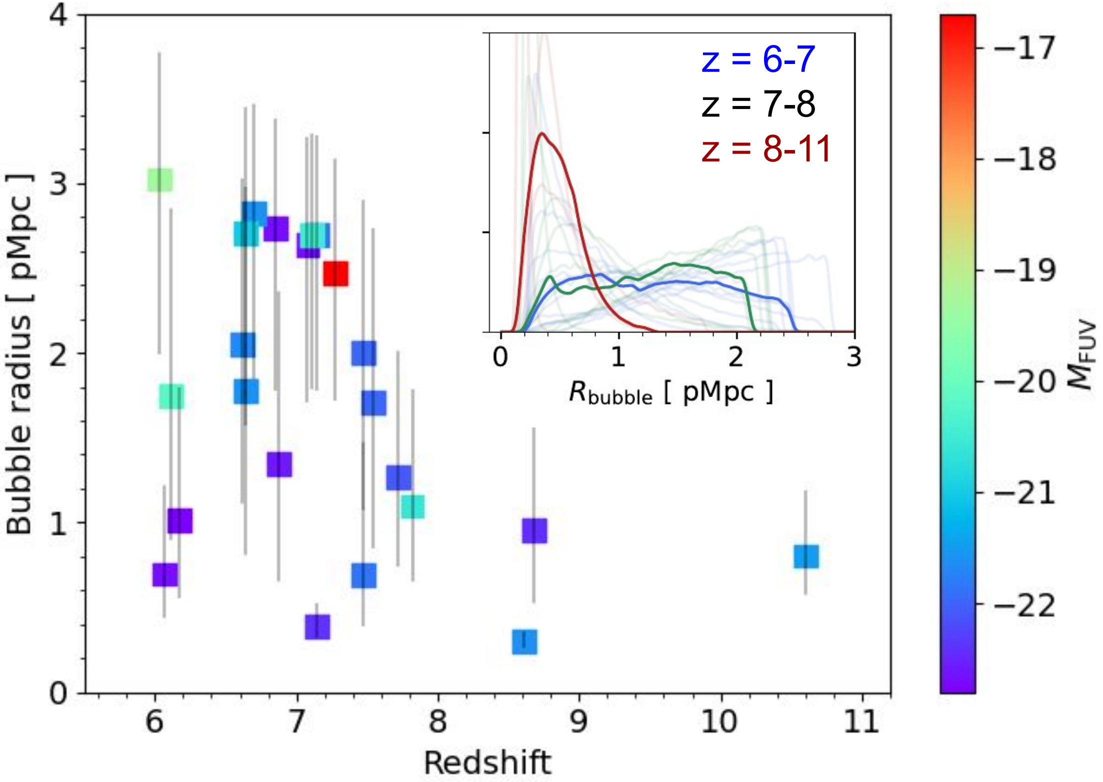

Bubble Size Distribution at z = 6 - 11

HII regions: **smaller at higher z**

N = 23 Κενδαλλ τ = -0.34 p = 0.02

10 – 90 % range of bubble sizes

N-body in 714 cMpc

RT with C^2-RAY

Less efficient $\chi_{\rm ion}$ Giri & Mellema 2022

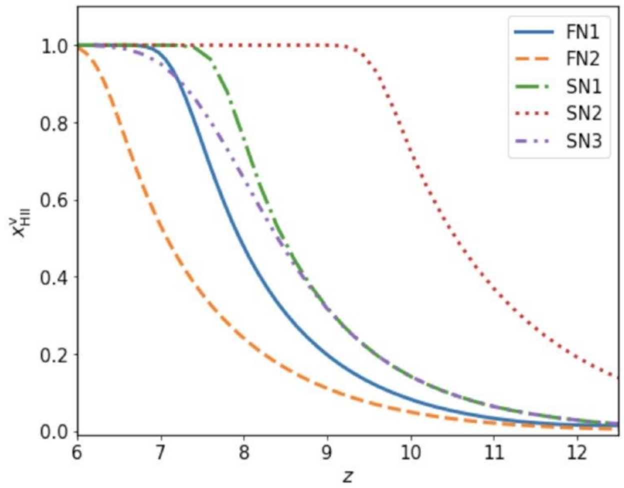

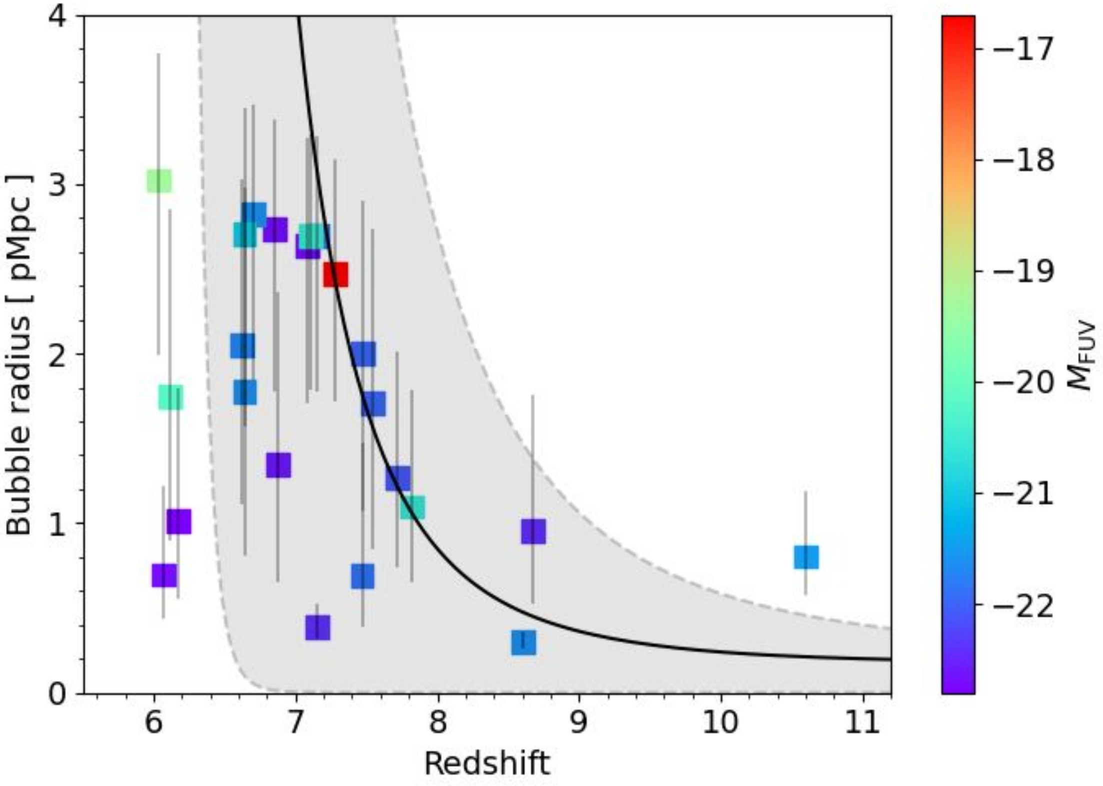

Ionizing Escape Fraction

$$R_{\mathrm{Strom}} = \left(\frac{3}{4\pi} \frac{Q_0}{n_{\mathrm{H}}^2 \alpha_{\mathrm{B}}} \right)^{1/3}$$

Ionizing Escape Fraction

$$R_{\mathrm{Strom}} = \left(\frac{3}{4\pi} \frac{Q_0}{n_{\mathrm{H}}^2 \alpha_{\mathrm{B}}} \right)^{1/3}$$

$$Q_0 = L_{\mathrm{UV}} \cdot \xi_{\mathrm{ion}} \cdot f_{\mathrm{esc}}$$

L_{UV} and ξ_{ion} known from observation

n_{H} known from cosmic baryon density

f is unknown

Ionizing Escape Fraction

$$R_{\text{Strom}} = \left(\frac{3}{4\pi} \frac{Q_0}{n_{\text{H}}^2 \alpha_{\text{B}}} \right)^{1/3}$$

$$Q_0 = L_{\text{UV}} \cdot \xi_{\text{ion}} \cdot f_{\text{esc}}$$

L_{UV} and ξ_{ion} known from observation

n_{H} known from cosmic baryon density

f is unknown

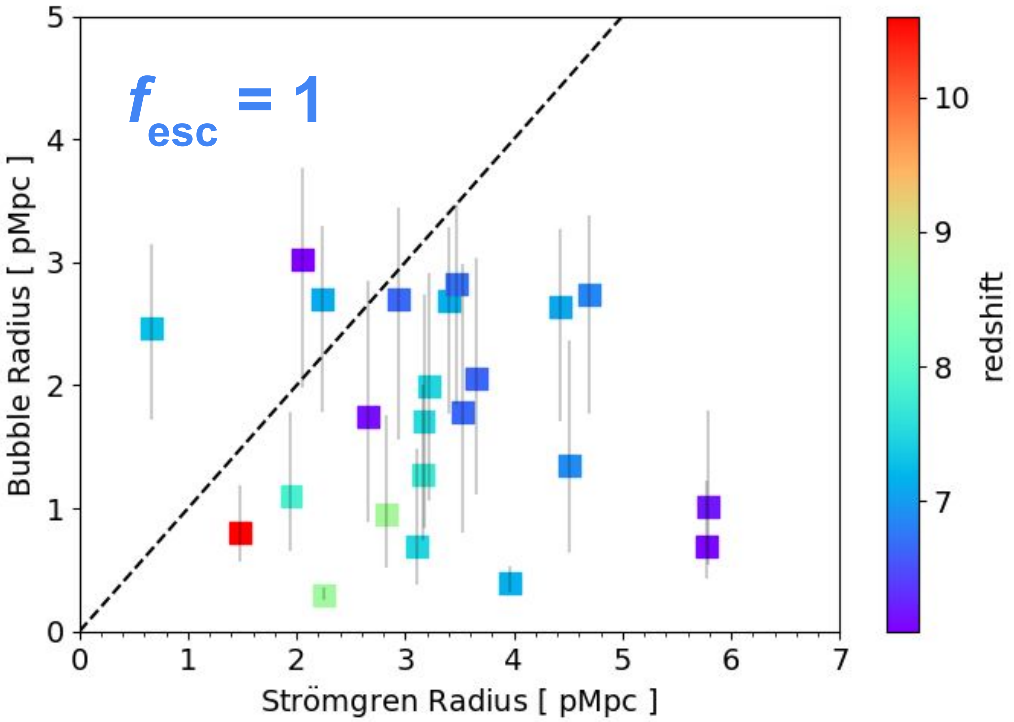

Ionizing Escape Fraction

$$R_{\mathrm{Strom}} = \left(\frac{3}{4\pi} \frac{Q_0}{n_{\mathrm{H}}^2 \alpha_{\mathrm{B}}} \right)^{1/3}$$

$$Q_0 = L_{\mathrm{UV}} \cdot \xi_{\mathrm{ion}} \cdot f_{\mathrm{esc}}$$

L_{UV} and ξ_{ion} known from observation

n_{H} known from cosmic baryon density

f is unknown

$$\rightarrow f_{\mathrm{esc}} = \left(\frac{R_{\mathrm{Bubble}}}{R_{\mathrm{Strom}}} \right)^3$$

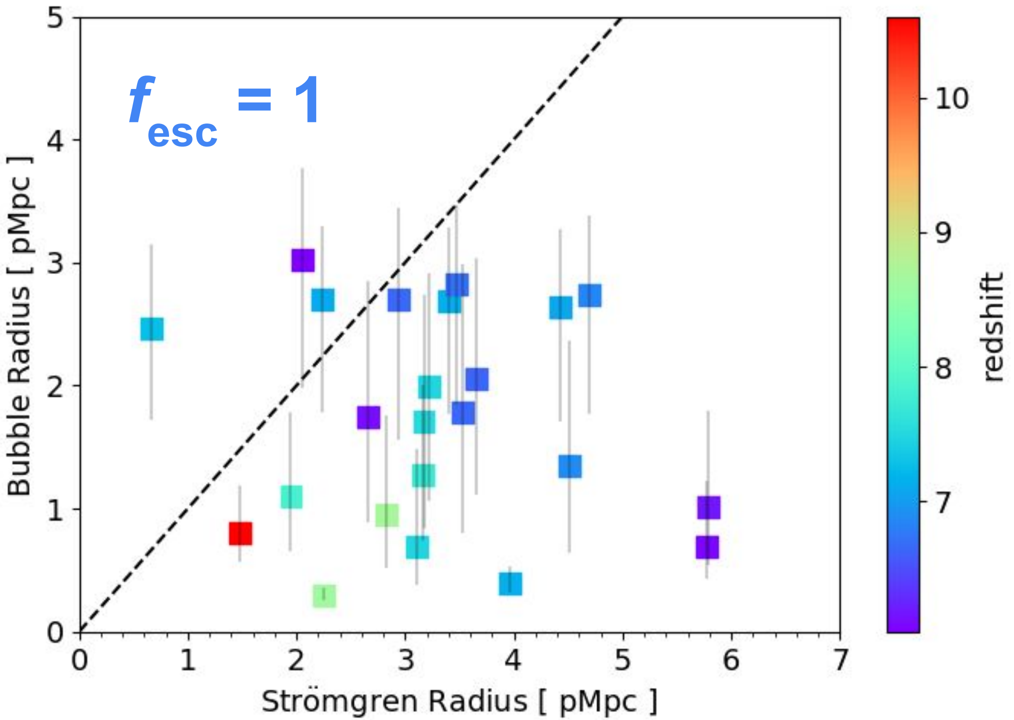

Ionizing Escape Fraction

$$R_{\mathrm{Strom}} = \left(\frac{3}{4\pi} \frac{Q_0}{n_{\mathrm{H}}^2 \alpha_{\mathrm{B}}} \right)^{1/3}$$

$$Q_0 = L_{\mathrm{UV}} \cdot \xi_{\mathrm{ion}} \cdot f_{\mathrm{esc}}$$

L_{UV} *and* ξ_{ion} known from observation

n_{H} known from cosmic baryon density

f is unknown

$$\rightarrow f_{\mathrm{esc}} = \left(\frac{R_{\mathrm{Bubble}}}{R_{\mathrm{Strom}}} \right)^3$$

f_{esc} median = 16%

68% range = 6 – 50 %

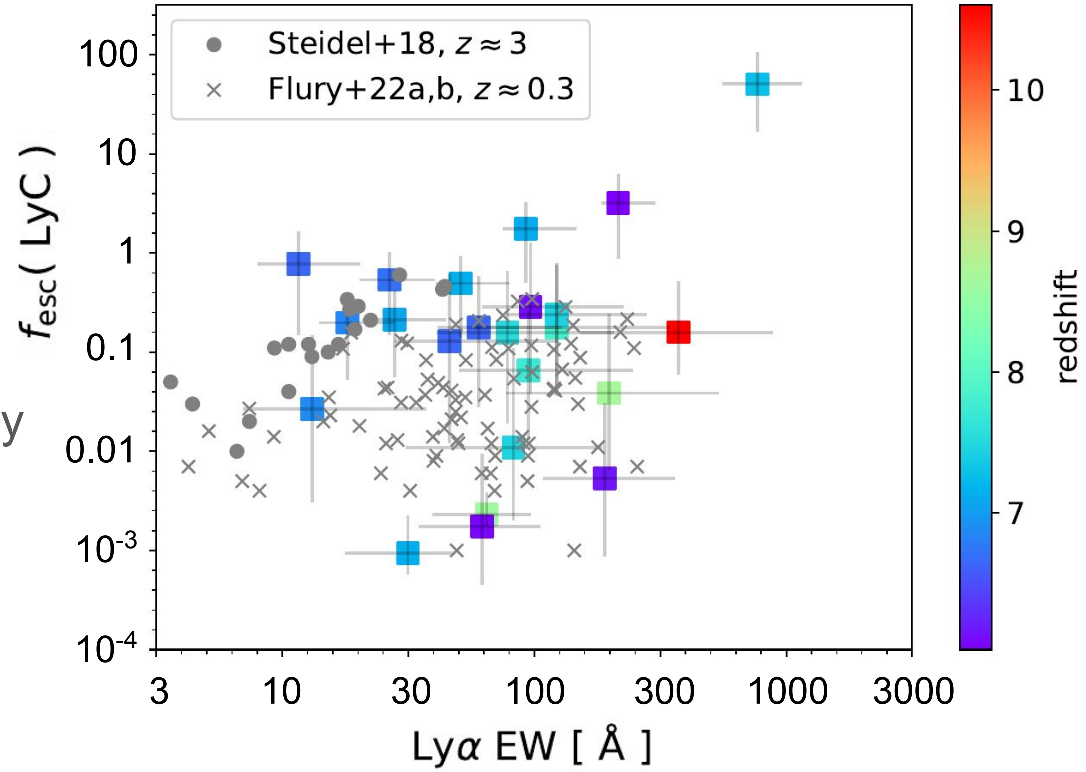

Ionizing Escape Fraction

$$R_{\mathrm{Strom}} = \left(\frac{3}{4\pi} \frac{Q_0}{n_{\mathrm{H}}^2 \alpha_{\mathrm{B}}} \right)^{1/3}$$

$$Q_0 = L_{\mathrm{UV}} \cdot \xi_{\mathrm{ion}} \cdot f_{\mathrm{esc}}$$

L_{UV} and ξ_{ion} known from observation

n_H known from cosmic baryon density

f is unknown

$$\rightarrow f_{\mathrm{esc}} = \left(\frac{R_{\mathrm{Bubble}}}{R_{\mathrm{Strom}}} \right)^3$$

f_{esc} median = 16%

68% range = 6 – 50 %

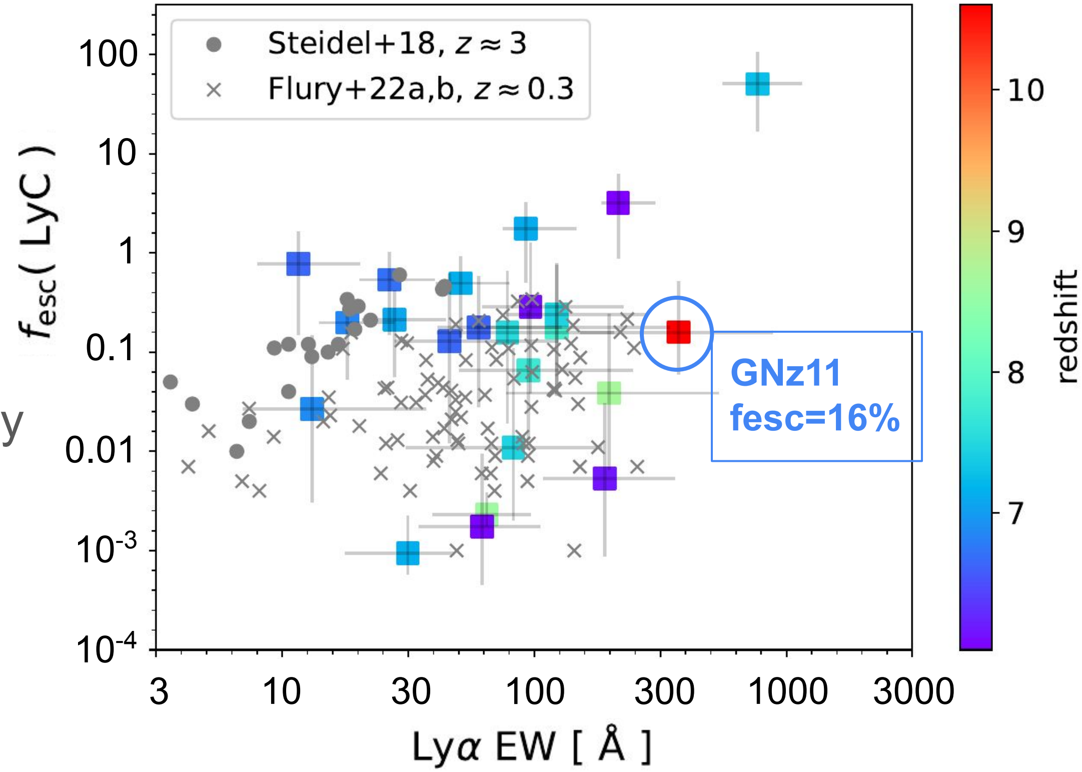

Conclusions

- Analyzed 87 galaxies observed with HST/COS and optical spectrographs
  Stellar modeling, nebular conditions, Lya profiles, etc.

- Lya is stronger in very young galaxies, likely due to photoionization feedback

- Absorbing envelope gets thicker as starburst continues, condensing more HI

- Low-z profiles (even z=0) CAN be used to make inferences at high-z

- Estimate sizes of HII regions in the EoR from Lya: 0.5 – 3 pMpc
  Bubbles grow from z=11 to 6

- Ionizing escape fractions at z=6-11 are 16 (6-50) %